TÜBİTAK

Turkish Journal of Earth Sciences

http://journals.tubitak.gov.tr/earth/

Research Article

Turkish J Earth Sci
(2018) 27: 349-383

doi:10.3906/yer-1710-24

Palynological and petroleum geochemical assessment of the Lower Oligocene Mezardere Formation, Thrace Basin, NW Turkey

Kadir GÜRGEY[1], **Zühtü BATI**[2,*]

[1]Department of Petroleum and Natural Gas Engineering, Near East University, Nicosia, Mersin 10, Turkey
[2]Turkish Petroleum Corporation (TPAO), Research and Development Center, Ankara, Turkey

Received: 31.10.2017 • **Accepted/Published Online:** 13.05.2018 • **Final Version:** 28.09.2018

Abstract: The Oligocene clastic sequence of the Mezardere Formation (MF) with laterally variable organic richness has long been known as a proven source of gas with minor oil accumulations across the Thrace Basin of northwest Turkey. However, based on well data for the thick MF, neither detailed work in relation to age dating and stratigraphy nor a close linkage between the depositional facies/environments, organic richness/organic proxies, and cyclicity has been established yet. In the present study, the MF was informally subdivided into Lower MF (LMF) and Upper MF (UMF) based on the distinct differences in palynological and geochemical data. Based on the common occurrences of *Glaphyrocysta* cf. *semitecta* and absence of *Wetzeliella gochtii*, the LMF is considered to be deposited during the earliest Oligocene (?Pshekian) under the prevailing marine conditions. The UMF is characterized by a very rich and diverse dinocyst assemblage having abundant occurrences of age-diagnostic *Wetzeliella gochtii* and a Solenovian age is assigned. Common *Pediastrum* occurrences in the UMF may suggest fresh water input as is the case for many source rocks of the Central and Eastern Paratethys. The UMF shows the geochemical characteristics of a typical transgressive sequence such as higher TOC, hydrogen index (HI), and relative hydrocarbon potential (RHP) values than those for the regressive LMF. On the RHP basis, three short-term transgressive to regressive cycles are recognized in the entire MF in the wells studied. The early mature UMF samples showed a fair to good source rock potential (average TOC = 1.14 wt. %; HI = 283 mg oil/g TOC) and low to moderate genetic petroleum potential (GP = 3.65 mg oil/g rock) and source potential index (SPI = 1.44 t oil/m^2). The LMF samples were not evaluated due to their apparently low TOC, HI, and S2 values. Better understanding of the MF will eventually aid a better understanding of the paleoenvironment of the Eastern Paratethys.

Key words: Thrace Basin, Lower Oligocene, *Wetzeliella gochtii*, transgression, regression, source rock

1. Introduction

During the Eocene/Oligocene transition, the Paratethys Ocean extending from France in Europe to Mangyshlak in inner Asia began to separate from the Tethys Ocean (Figures 1a–1c) (e.g., Rögl, 1999; Linda et al., 2003; Popov, 2004, 2010). The Lower Solenovian manganese ore deposits common in the Thrace Basin (Öztürk and Frakes, 1995; Gültekin, 1998) and in different areas of the Eastern Paratethys (Varentsov, 2002; Varentsov et al., 2003) have been considered to be clear evidence for a connection between the Thrace Basin and the Eastern Paratethys (Figure 1d). Similarity between the Lower Oligocene Mezardere oils of Western Turkey and Western Turkmenistan oils could be additional evidence that these oils are sourced from the Lower Oligocene source rocks deposited in the Eastern Paratethys (Figures 1a–1c) (Gürgey, 1999). Because of this and other reasons that will be discussed in the following sections, chronostratigraphic terms of the Eastern Paratethys (Figures 2a and 2b) are used throughout this study.

The gradual isolation of the Paratethys during the Pshekhian (Nannoplankton zones NP21/22) to Solenovian (NP23) may have caused the basin-wide occurrence of organic-rich sediments, deposited in a dysoxic–anoxic environment (Popov et al., 1993; Rögl, 1998, 1999) that constituted the active hydrocarbon source rocks in most parts of the Paratethys. The Maikop Group all over the Eastern Paratethys, particularly in the South Caspian Basin (Saint-Germes et al., 2000), the Menilite Formation in the Alpine Foreland Basin/Carpathians (Sachsenhofer et al., 2011), and the Ruslar Formation in the Kamchia Depression (Western Black Sea) onshore and offshore Bulgaria (Sachsenhofer et al., 2009; Bechtel et al., 2014) as well as the Tard Clay in the Pannonian Basin (Vetö, 1987; Bechtel et al., 2012) are good examples of organic-rich and active shale source rocks deposited in the Paratethys.

* Correspondence: bati@tpao.gov.tr

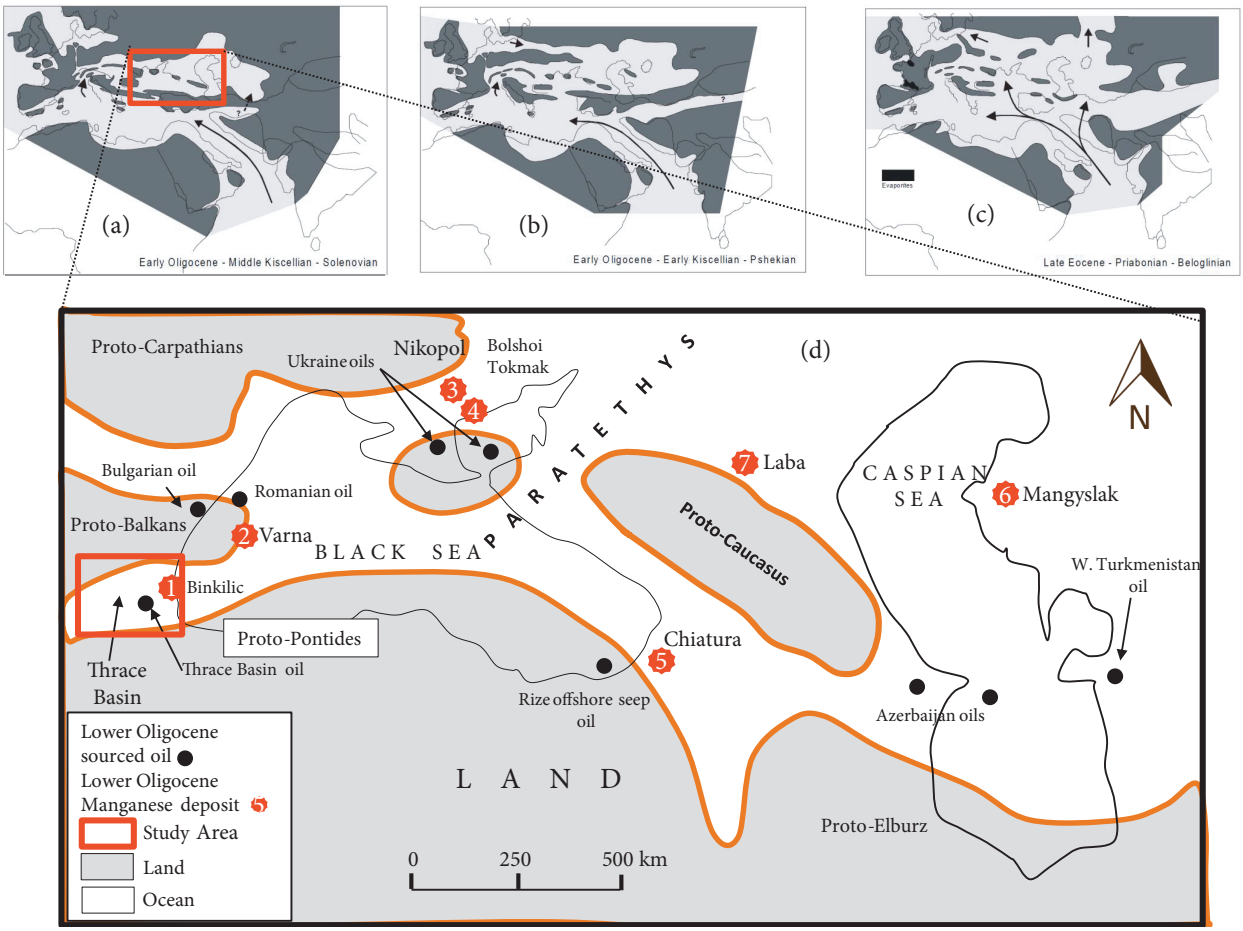

Figure 1. Maps showing (a) Isolated Eastern Paratethys from the Tethys Ocean in Solenovian, (b) Birth of the Eastern Paratethys from the Tethys Ocean in Pshekian, (c) A widespread Tethys Ocean in Beloglinian (Popov et al., 2004), and (d) Map showing the paleolocality of the Thrace Basin on the Eastern Paratethys during the Lower Oligocene (Robinson et al., 1996). The map also shows surface and subsurface occurrences of oils generated from Lower Oligocene source rocks (Gürgey, 1999) and Lower Oligocene aged manganese (Mn) deposit occurrences in the Eastern Paratethys including Binkılıç Mn deposits in the Thrace Basin (Öztürk and Frakes, 1995; Varentsov, 2002), which implies that the Thrace Basin following the Pshekhian belong to the Eastern Paratethys.

The Lower Oligocene Mezardere Formation from the Thrace Basin showing similar depositional history with the aforementioned Paratethys source rock examples is attributed to part of the Eastern Paratethys (Bati et al., 1993; Öztürk and Frakes, 1995; İslamoğlu et al., 2008; Bati, 2015).

The Eocene/Oligocene boundary in the Eastern Paratethys is characterized by a major sea level drop, which is followed by a subsequent sea level rise in the Rupelian (Popov et al., 2010). Turgut and Eseller (2000), based on the well log, core, outcrop, and biostratigraphic data and regional stratigraphic framework, have reported a major sea-level change and an occurrence of a long-term transgression during the Pshekian and Solenovian (Rupelian) (Figure 3). This appears to be the case, but our recent work and study on the geochemical proxies have indicated that there are also short-term fluctuations/cycles within this long-term transgression period proposed earlier by Turgut and Eseller (2000).

Petroleum potential of the Lower Oligocene Mezardere Formation in the Thrace Basin has been studied so far by several investigators. The authors in general pointed out that shales within the Mezardere Formation showed both conventional (Bürkan, 1992; Soylu et al., 1992) and unconventional shale-oil potential (Gürgey, 2015). However, the thickness of organic-rich interval/intervals (i.e. top and base levels) within the considerably thick (i.e. average thickness penetrated by the four wells used in this study is 1403 m; see Table 1) Mezardere Formation is still not known.

Most researchers have considered that transgressive intervals in general show high organic carbon content with marine amorphous type I and II organic matter

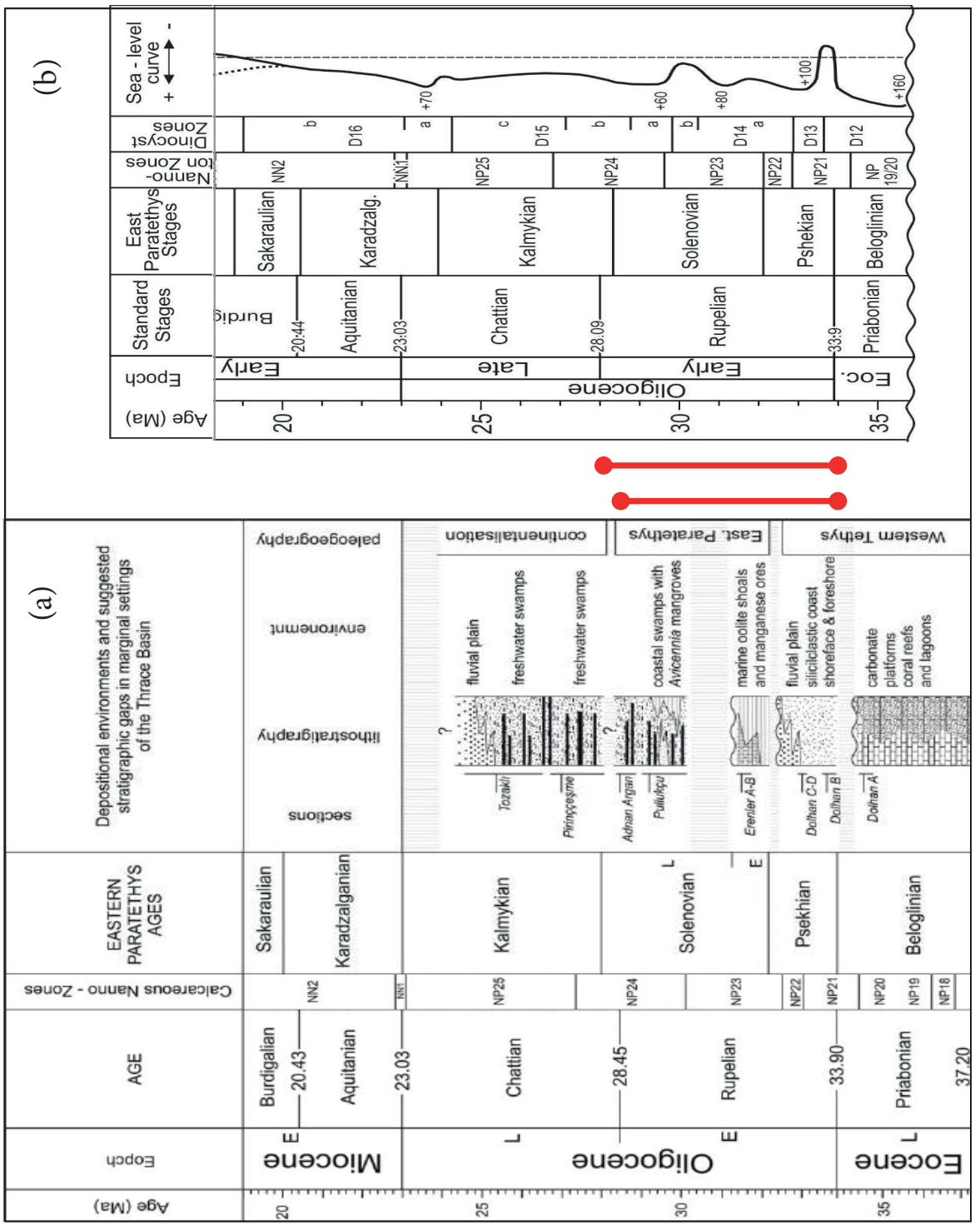

Figure 2. (a) Chronostratigraphic and nannoplankton biozonations (modified) of the Oligocene according to Gradstein et al. (2004). The Eastern Paratethys ages are adapted from Popov et al. (2004). Depositional environments, gaps in the measured sections in the Thrace Basin are given by İslamoğlu et al. (2008). (b) Chronostratigraphy, nannoplankton, dinocyst biozonations, and emphasized standard ages of the Eastern Paratethys Stages and relevant sea level curve during the Oligocene (Sachsenhofer et al., 2017).

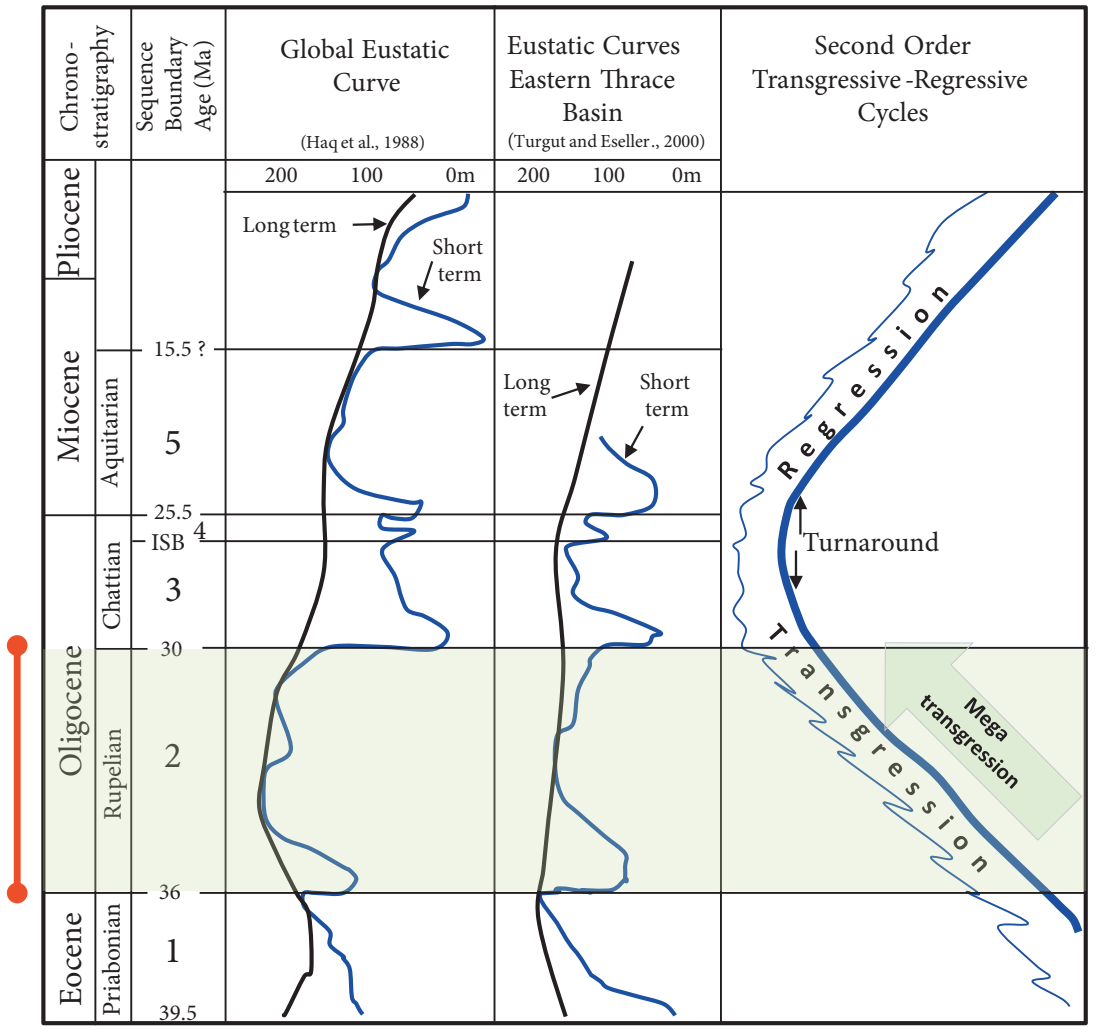

Figure 3. A model showing sea level curves for the Eastern Thrace Basin. As can be seen, a very slight difference exists between the Global Eustatic (Haq et al., 1988) and the regional Eastern Thrace Basin sea level curves (modified after Turgut and Eseller, 2000). An occurrence of mega-transgression during deposition of the Lower Oligocene (Rupelian) Mezardere Formation is noteworthy.

Table 1. Coordinates, top and base depths, and thickness of the Mezardere Formation for the four wells studied, Thrace Basin, NW Turkey. Well locations are given in Figure 4.

Well name	Easting	Northing	Top depth (m)	Base depth (m)	Thickness (m)
Karacaoglan-A (K-A)	270445.05	413338.01	1756	2835	1079
Kumrular-B (K-B)	271238.07	413035.04	1367	2625	1258
Umurca-C (U-C)	272619	412504	2164	3457	1293
Vakiflar-D (V-D)	273948	411554	1777	3760	1983
Average					1403

(Hart et al., 1994; Demaison and Moore, 1980; Jones, 1987; Creaney and Passey, 1993). Furthermore, the interrelationship between deposition of organic matter and existence of organic-rich units has been examined by Pasley et al. (1991) and Fang et al. (1993), and Omura and Hoyanagi (2004) showed once more that there is a strong

relationship between the transgressive deposits and organic richness (TOC) as well as hydrogen index (HI). They have stated that the sea level fluctuations, namely transgressive and regressive cycles, can be predicted by using geochemical proxies like TOC, HI, and relative hydrocarbon potential (RHP = S1 + S2/TOC) if the traditional biostratigraphic, seismic, and well log data are absent or limited (Curiale et al., 1992; Hart et al., 1994; Miceli-Romero and Philp, 2012; Abouelresh and Slatt, 2012; Slatt and Rodriguez, 2012; Freire and Monterio, 2013; Song et al., 2014).

The main purpose of the present paper is to subdivide the considerably thick Mezardere Formation into meaningful and correlatable zones/cycles with the help of dinocyst assemblages that have not been studied in detail yet. The second aim is to determine the nature of rising (transgressive) and falling (regressive) sea level cycles by using geochemical proxies such as TOC, HI, and RHP. The third objective is to evaluate the source and the hydrocarbon potential of selected organic-rich units (ORUs) from the transgressive intervals. Along with all these above, the paleoenvironmental evolution of the Lower Oligocene Mezardere Formation during 33.9–28.09 m.y. interval (see Figure 2a) (İslamoğlu et al., 2008) (Figure 2b) (Sachsenhofer et al., 2017) has been also addressed in this study. The locations of 4 wells from which the samples were collected are shown in Figure 4.

2. Geologic overview

2.1. Petroleum geology

The basin structural geology and tectonic history (Perinçek, 1991), stratigraphy and in part related sedimentology (Turgut et al., 1991; Turgut and Eseller, 2000; Siyako and Huvaz, 2007), and petroleum geochemistry (Gürgey et al., 2005; Hoşgörmez et al., 2005; Gürgey, 2014, 2015) under the petroleum geology can be found in the several papers above so far published in the Thrace Basin. Since the beginning of early hydrocarbon exploration in 1934, more than 660 conventional wells targeting oil and gas have been drilled across the basin. As a consequence, along with the 13MM bbl oil in-place, significant volume (some 12 Bm^3 in-place) of conventional natural gas has been discovered in the basin. The proven hydrocarbon source bed, the Mezardere Formation, shows large variations in both TOC and HI values in both lateral and vertical directions. The 407 Mezardere Formation samples analyzed from 47 wells indicate that TOC ranges from 0.08 to 3.39 wt. % and averages around 0.86 wt. % (i.e. Std Dev. = 0.46 wt. %). Similarly, HI ranges from 3 to 744 mg HC/g TOC and averages 185 mg HC/g TOC (i.e. Std Dev. = 122 mg HC/g TOC). Considerable discussion and relevant evaluation pertaining to the Mezardere Formation source rock and its character can be found in the published papers (Gürgey, 2013). Correlation studies in relation to oil to source rock (Gürgey, 2014) and wet gas/condensate to source rock have revealed that the Mezardere Formation was the source rock of the crude oil and wet-gas/condensate in the Gelindere and Değirmenköy fields, respectively (Gürgey et al., 2005) (see Figure 4 for location of the fields).

2.2. Stratigraphy and paleodepositional setting

Generalized stratigraphy of the Tertiary Thrace Basin is shown in Figure 5. The older rocks underlying the Lower Oligocene Mezardere Formation are the shallow marine uppermost Eocene/Priabonian sediments. An erosional contact exists between the Mezardere Formation unconformably underlain by the Ceylan Formation (Erten and Çubukçu, 1988). It is conformably overlain by the Osmancık Formation (Figure 5). The Lower Oligocene Mezardere Formation is a laterally extensive unit (22,335 km^2) and covers the entire Thrace Basin. It consists of interbedded greenish gray to green shales, siltstones, marlstones, and fine-grained sandstones. Tuffaceous interbeds are also intermittently present in the very lower part of the formation. The greenish and gray shales generally contain abundant organic matter (Turgut et al., 1991). The sandstone-dominated interval is named the Teslimköy Member. Thickness of the Mezardere Formation is 1540 m in the type section at Yenimuhacir village (Siyako, 2006) (see Figure 2 for location). However, seismic and well data reveal that it reaches up to 2500 m in the subsurface. Furthermore, its widespread outcrops are found in the southwestern part of the basin within the area as a trend from Keşan-Malkara to the city of Tekirdağ (Siyako, 2006) (Figure 4). On the basis of palynologic studies, a Late Eocene–Early Oligocene age was assigned for the Mezardere Formation (Ediger and Alişan, 1989; Bati et al., 1993).

Whether the Early Oligocene sea of the Thrace Basin in which the Mezardere clastics were laid down belongs to either Tethys or Eastern Paratethys has long been a discussion in the literature (İslamoğlu et al., 2008). The Lower Oligocene (Lower Solenovian) manganese (Mn) occurrences of ore deposits at Binkılıç in the Thrace Basin have been reported by Öztürk and Frakes (1995), Gültekin (1998), Varentsov (2002), and Varentsov et al. (2003) (Figure 1d). The Mn deposits of the Thrace Basin are at least intermittently coeval and connected with the other Mn deposits (i.e. Mn deposits in the Varna region in Bulgaria, Nikopol in Ukraine, Chiatura in Georgia, and Mangyshlak in Kazakhstan (Figure 1d)) reported in the Paratethys (Varentsov, 2002; Varentsov et al., 2003; İslamoğlu et al., 2008). This observation supports the consideration that the Mezardere Formation is most likely formed in the Paratethys Ocean (Öztürk and Frakes, 1995; İslamoğlu et al., 2008). Sachsenhofer et al. (2009), in their work in the Oligocene Ruslar Formation (Kamchia Depression,

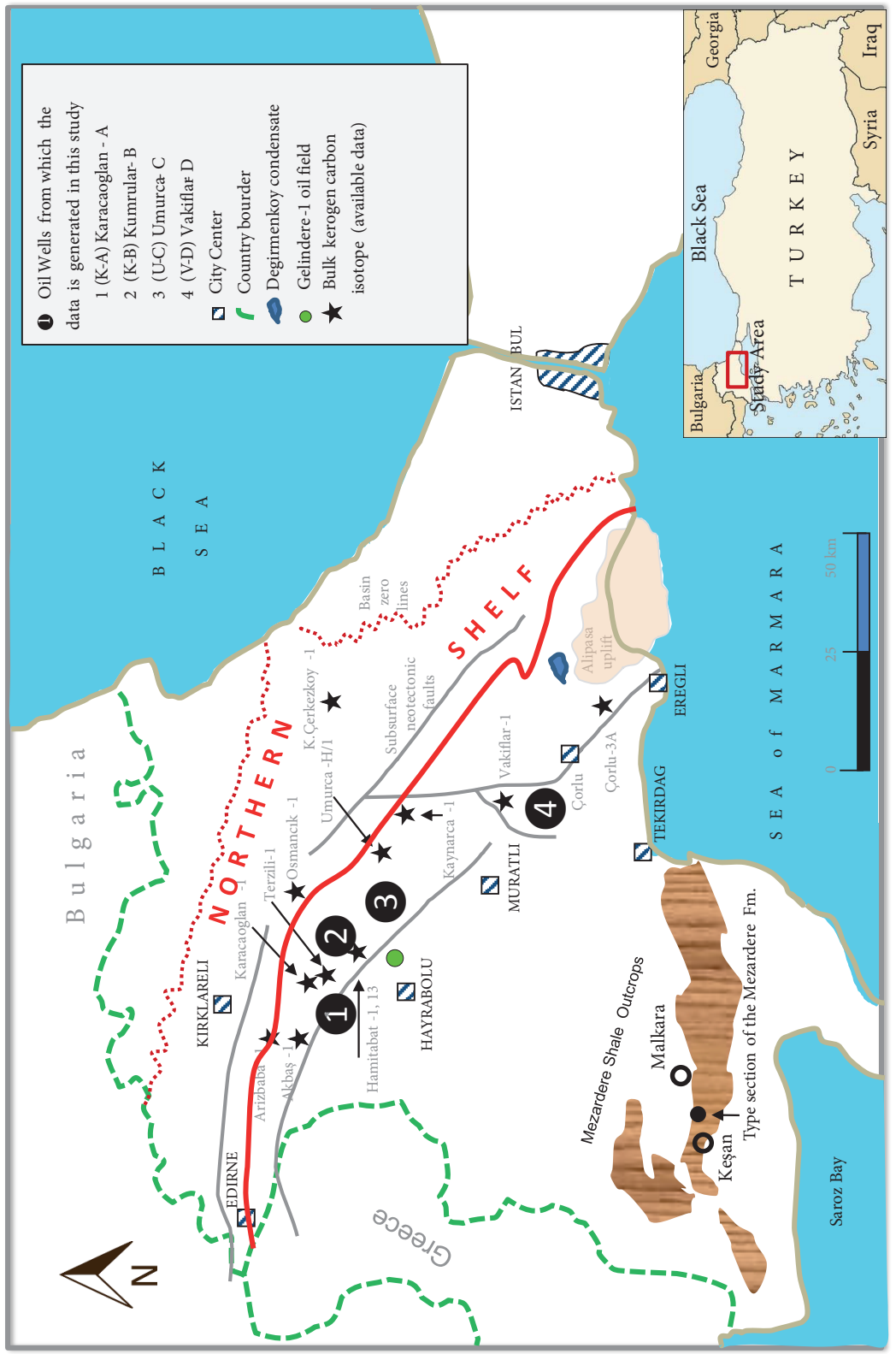

Figure 4. Map showing the localities of the studied four wells namely, K-A, K-B, U-C, and V-D, in the Thrace Basin, NW Turkey. Shaded areas in the southwestern portion of the basin indicate outcrop exposures of the Lower Oligocene Mezardere Formation.

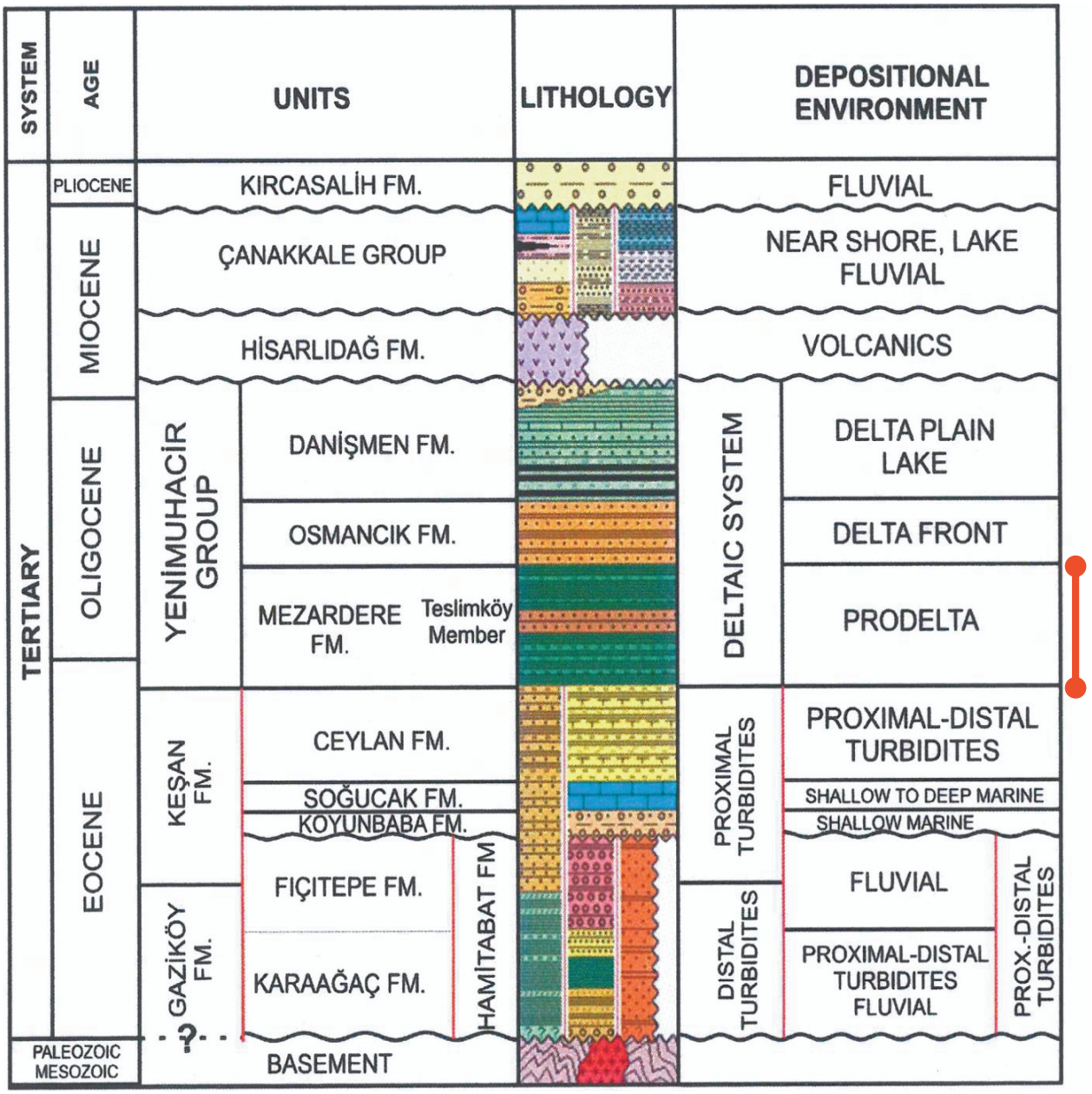

Figure 5. Generalized stratigraphy of the Thrace Basin showing lithology and depositional environments of the formations (Siyako, 2006; Sünnetçioğlu, 2008).

Western Black Sea) simplified the Early Oligocene paleogeographic map of the Paratethys prepared by Popov et al. (2004) and divided the Paratethys into two as Eastern Paratethys and Western + Central Paratethys. Similarly, they simplified the chronostratigraphic scheme prepared by Popov and Stolyarov (1996) for the Eastern and Central Paratethys area and gave the correlation of local stages with Mediterranean stages and calcareous nannoplankton zones. In the simplified Oligocene paleogeographic map by Sachsenhofer et al. (2009), the Thrace Basin is also located in the western part of the Eastern Paratethys. This also implies that the Thrace Basin was one of the subbasins in the Eastern Paratethys during the Early Solenovian time when the Eastern Paratethys became isolated from the Tethys Ocean and the Mezardere Formation is most likely deposited in this subbasin. This gave us confidence to use the regional Eastern Paratethys sea level curve of Popov et al. (2010) and his chronostratigraphic stages instead of using the global eustatic sea level curve of Haq et al. (1987) (Figures 2a and 2b).

3. Samplings and analytical methods

3.1 Sample collection and treatment

For the analysis, a total of 113 selected shale samples were collected from the four wells. The well names, Karacaoglan-A (K-A), Kumrular-B (K-B), Umurca-C (U-C), and Vakiflar-D (V-D), and well localities are given in Figure 4. Detailed information about the wells is given in Table 1. The wells were selected from the shelf area of the Thrace Basin in order to see a better resolution in sea level fluctuations while they are examined by potential sea level indicators of geochemical proxies.

Distribution of the total 102 Rock-Eval samples analyzed with referring to the studied wells, K-A, K-B, U-C, and V-D, is 14, 17, 18, and 53, in number, respectively. Twenty-nine samples were studied for maceral analyses and 26 samples were analyzed for vitrinite reflectance (% Ro) measurements. There is one additional subset of data of the analysis: 31 independently selected composite samples from the four wells were examined palynologically.

In the present study, the liquid hydrocarbon contaminated and mature–overmature samples were initially dismissed. Therefore, the samples that were contaminated or mature–overmature were not considered for further evaluation.

3.2. Analytical methods

3.2.1. Palynological sample processing and analyses

Palynological preparations from the composite well cuttings were processed at the Turkish Petroleum Corporation (TPAO) Research and Development Center Laboratories in Ankara, following the standard laboratory techniques the details of which were given in Bati (1996). Simply, following disaggregation and cleaning, the samples were first treated with HCl (33%) to remove the carbonates and then with HF (40%) to remove the silicates. Following acid treatments, heavy liquids ($ZnCl_2$) were used to separate the light organic fraction from the heavier fraction. Finally, organic residue was sieved at 200 μm and either 20 or 10 μm and mounted in glycerin jelly for light microscope observation. All samples were qualitatively and semiquantitatively analyzed, microphotographs of the selected taxa were taken, and two plates were prepared to illustrate some of the selected taxa (Figures 6a–6l and 7a-7l).

3.2.2. Rock-Eval pyrolysis

Pyrolysis measurements were performed using a Rock-Eval-II pyrolysis instrument under the standard conditions described by Peters (1986) and are presented in Table 2. Generated S1 and S2 (mg HC/g rock) peak values were measured, and the S2 peak was used to calculate both the hydrogen index (HI = (S2 × 100/TOC) mgHC/gTOC) and production index (PI = (S1 + S2)/S1) (Barker, 1974). The temperature at the S2 peak maximum is used for Tmax recorded as a maturity parameter. Tmax values were later converted to % VRcal (calculated vitrinite reflectance) using the equation proposed by Jarvie et al. (2001): % VRcal = 0.018 × Tmax – 7.16). TOC was determined as the sum of the carbon in the pyrolyzate plus the carbon from the residual oxidized organic matter.

In the present study, Rock-Eval data were used for two main purposes: 1) to examine sea level fluctuations by using proxies such as TOC, HI, and RHP, and 2) to evaluate selected ORUs from the Mezardere Formation for their hydrocarbon potential.

3.2.3. Incident light microscopy

Maceral percentages of the Mezardere Formation samples are determined on carefully prepared kerogen smear slides by Zeiss Axipolan incident light petrographic microscope (Harput and Gökçen, 1991). Standard palynological techniques are applied for kerogen isolation and smear slide preparation. Four maceral components were recognized in kerogen slides: i) AOM % (amorphous/algal-aquatic phytoplankton-dinocysts, acritarchs etc. including their degraded amorphous products), ii) HSP % (herbaceous- mainly terrestrial types of kerogen- spore, pollen, cutinite, and membranes) iii) W % (woody parts of wood stems and branches), and iv) C % (coaly-oxidized metamorphosed carbon particles) (Harput and Gökçen, 1991). A total of 29 kerogen smear slides were examined for maceral analysis: K-A = 9, K-B = 5, U-C = 7, and V-D = 8 samples. At the same time, vitrinite reflectance (% Ro) measurements were conducted on 26 kerogen smear slide samples containing autochthonous vitrinite particles.

All the analyses were conducted at the Turkish Petroleum Corporation Research and Development Center Laboratories in Ankara, Turkey.

3.2.4. Statistical analyses

The software WinsTAT for Excel was used for the statistical treatment of the data. Firstly, using this software the descriptive statistics (e.g., mean, standard deviation, minimum, and maximum) of the organic geochemical and petrographical parameters were obtained. Secondly, Pearson's correlation coefficients (PCCs) between the organic geochemical and petrographical parameters were calculated. The PCC is the test statistics that measures the statistical relationship, association, between two continuous and linear variables. It is known to be the best method of measuring the association between parameters of interest: coefficient values can range from +1 to –1, where +1 indicates a perfect positive relationship, –1 indicates a perfect negative relationship, and 0 indicates no relationship exists.

4. Results

In the present study, several analyses are conducted and subsequently used in the interpretation. These are namely

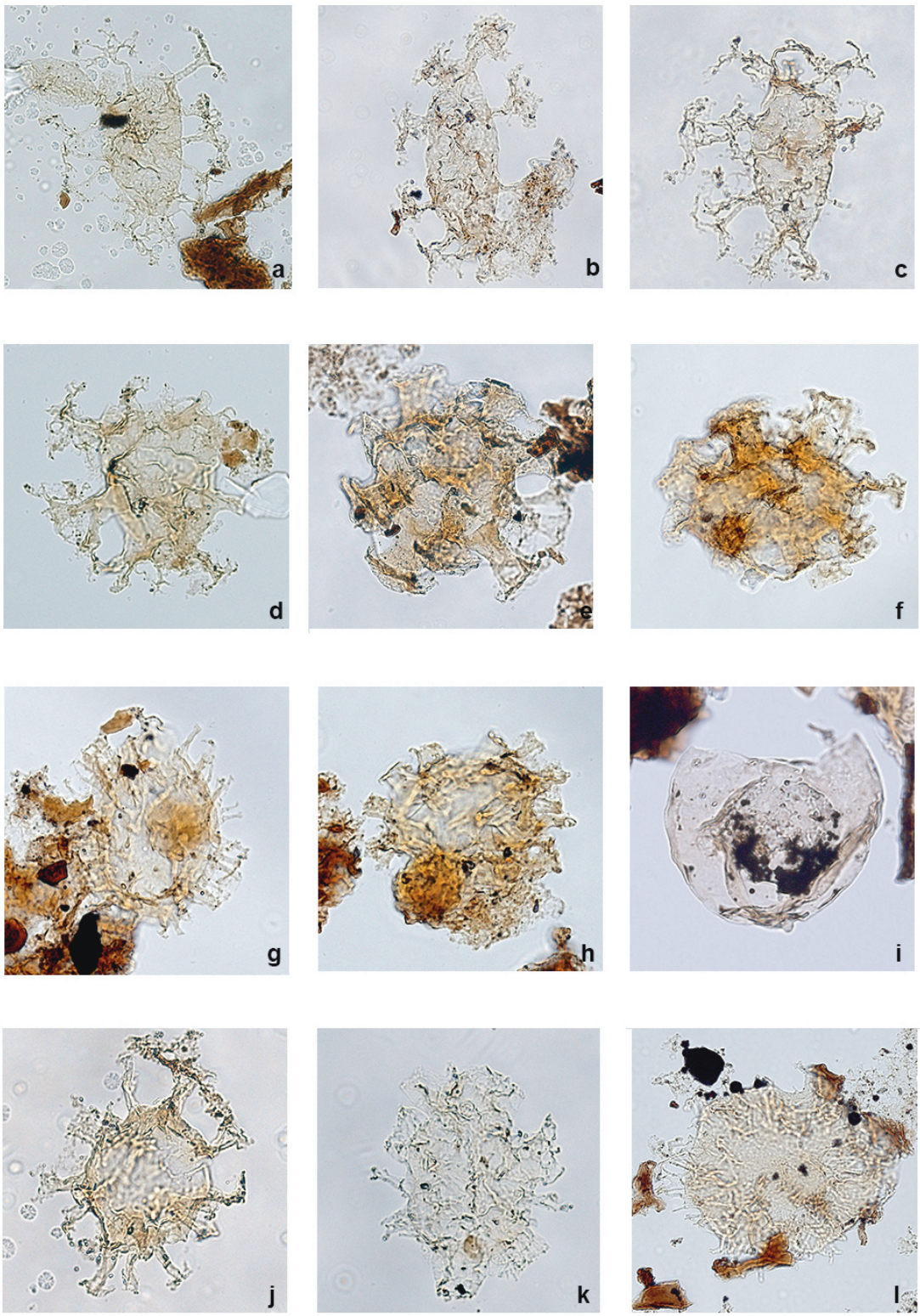

Figure 6. (a) *Distatodinium ellipticum*, K-B, 2222–2230 m, 86.5 µm, (b) *Distatodinium ellipticum*, K-A, 2140–2148 m, 111.0 µM, (c) *Distatodinium ellipticum*, K-A, 2140–2148 m, 90.8 µm, (d) *Distatodinium craterum*, K-A, 2206–2214 m, 72.0 µm, (e) *Cordosphaeridium cantharellus*, K-A, 2348–2358 m, 111.0 µm, (f) *Cordosphaeridium fibrospinosum*, K-A, 2140–2148 m, 100.9 µm, (g) *Polysphaeridium zoharyii*, K-A, 2140–2148 m, 64.8 µm, (h) *Homotryblium vallum*, K-A, 2140–2148 m, 61.9 µm, (i) *Batiacasphaera explanata*, K-B, 2828 m, 61.9 µm, (j) *Homotryblium plectilum*, K-A, 2140–2148 m, 96.5 µm, (k) *Hystrichokolpoma cinctum*, K-A, 2140–2148 m, 69.1 µm, (l) *Cleistosphaeridium placacanthum*, K-B, 2080 m, 100.9 µm.

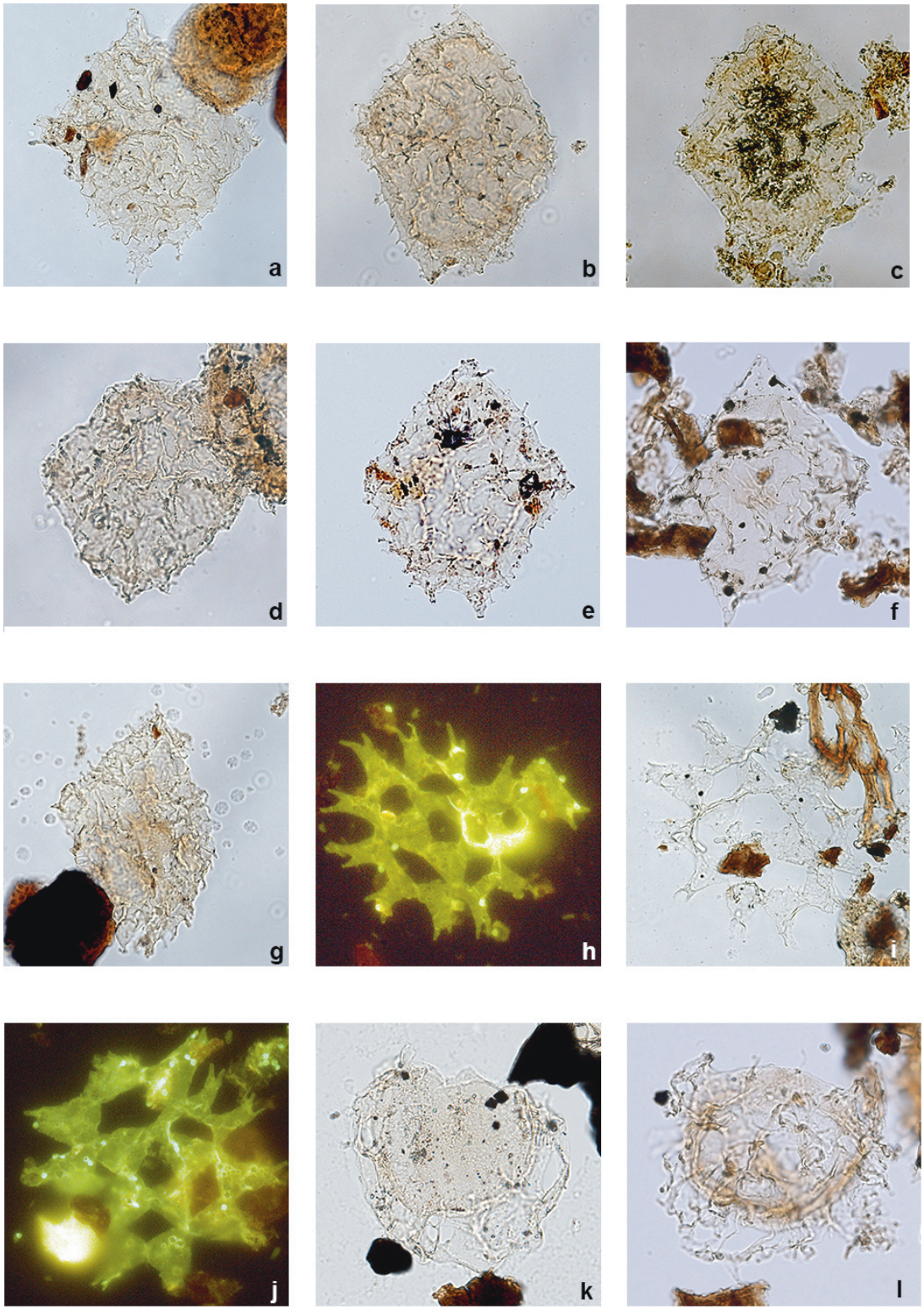

Figure 7. (a) *Wetzeliella symmetrica*, K-A, 2206–2214 m, 141.0 µm, (b) *Wetzeliella gochtii*, U-C, 2860 m, 111.0 µm, (c) *Wetzeliella gochtii*, K-A, 2140–2148 m, 101.0 µm, (d) *Wetzeliella gochtii*, K-B, 1960 m, 93.7 µm, (e) *Wetzeliella gochtii*, K-A, 2206–2214 m, 96.6 µm, (f) *Wilsonidium ornatum*, K-A, 2140–2148 m, 111.0 µm, (g) *Wetzeliella ovalis,* K-A, 2140–2148 m, 115.3 µm, (h) *Pediastrum* sp., V-D, 2618–2658 m, 96.6 µm, (i) *Pediastrum* sp., V-D, 2618–2658 m, 108.1 µm, (j) *Pediastrum* sp., V-D, 2618–2658 m, 122.5 µm, (k) *Glaphyrocysta* cf. *semitecta*, K-B, 2222–2230 m, 47.7 µm, (l) *Glaphyrocysta* sp., K-A, 2140–2148 m, 72.1 µm.

Table 2. Results showing Rock-Eval analysis (taken from Gürgey, 2015) and incident light microscopy of the Mezardere Formation samples. Note that Lower Mezardere Formation (LMF) samples and Upper Mezardere Formation (UMF) samples are listed separately. Well locations are given in Figure 4 and descriptions of the parameters that are used throughout the study are as follows: Depth = the depth samples were taken from (m); TOC = total organic carbon (wt.%); Tmax = the temperature at which max. hydrocarbon yield occurs at pyrolysis S2 peak (°C); HI = hydrogen index = S2 × 100/TOC (mg HC/g rock); S1 = free volatile hydrocarbons thermally flushed from a rock sample at 300 °C (mg HC/g rock); S2 = hydrocarbons cracked from solid kerogen under standard pyrolysis temperature (mg HC/g rock); GP = genetic potential = S1 + S2 (mg HC/g rock); PI = production index = S1/S1 + S2; OSI = oil saturation index = S1 × 100/TOC; RHP = relative hydrocarbon potential = (S1 + S2)/TOC (Fang et al., 1993); Vrcal = calculated vitrinite reflectance = 0.018 × Tmax – 7.16 (%) (Jarvie et al., 2001); HOM = herbaceous + spore + pollen organic matter in a kerogen slide (%); AOM = alginite + amorphous organic matter in a kerogen slide (%); WOM = woody (terrestrial) organic matter in a kerogen slide (%); COM = coaly (terrestrial) organic matter in a kerogen slide (%); W+C OM = WOM + COM (%); % Ro = Measured vitrinite reflectance in the laboratory (%)

				Organic geochemistry									Organic petrography							
SN	WName	Zone	Depth	TOC	Tmax	HI	S1	S2	GP	PI	OSI	RHP	VRcal	HOM	AOM	WOM	COM	W+C	%Ro	
1	K-A	UMF	1850	1.23	427	413	0.13	5.09	5.22	0.02	11	4.24	0.53	20	30	50	0	50	0.50	UMF (UPPER MEZARDERE FORMATION)
2	K-A	UMF	2096	0.60	439	90	0.03	0.58	0.61	0.05	5	1.02	0.74	30	40	30	0	30	0.50	
3	K-A	UMF	2122	0.94	437	195	0.10	1.84	1.94	0.05	11	2.06	0.71							
4	K-A	UMF	2130	1.21	433	414	0.23	5.01	5.24	0.04	19	4.33	0.63							
5	K-A	UMF	2346	0.61	438	121	0.04	0.73	0.77	0.05	7	1.26	0.72	30	30	40	0	40	0.55	
6	K-B	UMF	1440											15	65	20	0	20	0.44	
7	K-B	UMF	1510	1.34	430	288	0.12	3.87	3.99	0.03	9	2.98	0.58							
8	K-B	UMF	1550	1.44	432	263	0.10	3.79	3.89	0.03	7	2.70	0.62							
9	K-B	UMF	1690	1.61	434	443	0.29	7.15	7.44	0.04	18	4.62	0.65	15	65	20	0	20	0.46	
10	K-B	UMF	1730	1.86	434	728	0.37	13.55	13.92	0.03	20	7.48	0.65							
11	K-B	UMF	1760	1.65	435	744	0.43	12.28	12.71	0.03	26	7.70	0.67							
12	K-B	UMF	1830	1.32	435	132	0.33	3.07	3.40	0.10	25	2.57	0.67							
13	K-B	UMF	1890	1.32	435	280	0.38	3.70	4.08	0.09	29	3.09	0.67							
14	K-B	UMF	1930	1.72	430	347	0.71	5.96	6.67	0.11	41	3.88	0.58							
15	K-B	UMF	1950											15	40	35	10	45	0.49	
16	K-B	UMF	1970	1.54	436	545	0.51	8.40	8.91	0.06	33	5.79	0.69							
17	K-B	UMF	2020	1.31	431	400	0.36	5.25	5.61	0.06	27	4.28	0.60							
18	U-C	UMF	2190	1.43	429	224	0.09	3.21	3.30	0.03	6	2.31	0.56							
19	U-C	UMF	2200	0.96	435	67	0.02	0.64	0.66	0.03	2	0.69	0.67							
20	U-C	UMF	2240	1.23	432	118	0.08	1.45	1.53	0.05	7	1.24	0.62							
21	U-C	UMF	2270	1.04	434	289	0.05	3.00	3.05	0.02	5	2.93	0.65							
22	U-C	UMF	2290	1.43	436	327	0.10	4.67	4.77	0.02	7	3.34	0.69							
23	U-C	UMF	2320											30	55	10	5	15	0.50	
24	U-C	UMF	2368	0.86	429	149	0.06	1.28	1.34	0.04	7	1.56	0.56							
25	U-C	UMF	2430	0.92	430	121	0.08	1.12	1.20	0.07	9	1.30	0.58							
26	U-C	UMF	2500	1.17	429	140	0.08	1.64	1.72	0.05	7	1.47	0.56							
27	U-C	UMF	2560											35	25	30	10	40	0.52	
28	U-C	UMF	2630	0.92	431	236	0.11	2.17	2.28	0.05	12	2.48	0.60							
29	U-C	UMF	2640	1.12	431	208	0.20	2.33	2.53	0.08	18	2.26	0.60							
30	U-C	UMF	2690	0.84	434	184	0.14	1.55	1.69	0.08	17	2.01	0.65							
31	U-C	UMF	2720	0.77	439	190	0.01	1.95	1.96	0.01	1	2.55	0.74							
32	U-C	UMF	2750	1.23	434	76	0.10	0.94	1.04	0.10	8	0.85	0.65	40	30	20	10	30	0.53	
33	U-C	UMF	2860	0.99	434	221	0.10	2.19	2.29	0.04	10	2.31	0.65	40	30	20	10	30	0.60	
34	V-D	UMF	2013	0.79	429	69	0.02	0.54	0.56	0.04	3	0.71	0.56							
35	V-D	UMF	2059	1.12	430	229	0.15	2.56	2.71	0.06	13	2.42	0.58							
36	V-D	UMF	2104	1.47	426	289	0.12	4.26	4.38	0.03	8	2.98	0.51							
37	V-D	UMF	2151	1.28	436	237	0.09	3.04	3.13	0.03	7	2.45	0.69							

Table 2. (Continued).

				Organic geochemistry									Organic petrography							
SN	WName	Zone	Depth	TOC	Tmax	HI	S1	S2	GP	PI	OSI	RHP	VRcal	HOM	AOM	WOM	COM	W+C	%Ro	
38	V-D	UMF	2164											30	20	35	15	50	0.50	UMF (UPPER MEZARDERE FORMATION)
39	V-D	UMF	2181	0.81	431	89	0.04	0.72	0.76	0.05	5	0.94	0.60							
40	V-D	UMF	2210	1.12	432	310	0.04	3.47	3.51	0.01	4	3.13	0.62							
41	V-D	UMF	2226	1.14	421	257	0.02	2.93	2.95	0.01	2	2.59	0.42							
42	V-D	UMF	2241	1.07	427	216	0.06	2.31	2.37	0.03	6	2.21	0.53							
43	V-D	UMF	2271	1.07	427	579	0.24	6.20	6.44	0.04	22	6.02	0.53							
44	V-D	UMF	2287	1.02	428	257	0.09	2.75	2.84	0.03	9	2.78	0.54							
45	V-D	UMF	2302	0.93	428	363	0.07	3.37	3.44	0.02	8	3.70	0.54							
46	V-D	UMF	2357	1.14	427	504	0.10	5.75	5.85	0.02	9	5.13	0.53							
47	V-D	UMF	2390	1.34	434	530	0.09	7.10	7.19	0.01	7	5.37	0.65							
48	V-D	UMF	2438	0.95	430	293	0.40	2.78	3.18	0.13	42	3.35	0.58	30	20	35	15	50	0.50	
49	V-D	UMF	2439	0.95	430	293	0.04	2.78	2.82	0.01	4	2.97	0.58							
50	V-D	UMF	2454	1.17	428	457	0.13	5.35	5.48	0.02	11	4.68	0.54							
51	V-D	UMF	2470	1.23	423	603	0.20	7.41	7.61	0.03	16	6.19	0.45							
52	V-D	UMF	2531	1.20	426	404	0.22	4.85	5.07	0.04	18	4.23	0.51							
53	V-D	UMF	2576	1.10	429	368	0.16	4.05	4.21	0.04	15	3.83	0.56							
54	V-D	UMF	2598	1.20	430	356	0.15	4.27	4.42	0.03	13	3.68	0.58							
55	V-D	UMF	2616	1.10	431	165	0.14	1.81	1.95	0.07	13	1.77	0.60							
56	V-D	UMF	2683	1.11	431	184	0.31	2.05	2.36	0.13	28	2.13	0.60							
57	V-D	UMF	2698	1.10	429	209	0.16	2.30	2.46	0.07	15	2.24	0.56							
58	V-D	UMF	2713	1.48	430	280	0.21	4.14	4.35	0.05	14	2.94	0.58							
59	V-D	UMF	2728	1.05	427	187	0.16	2.30	2.46	0.07	15	2.34	0.53	45	30	20	5	25	0.50	
60	V-D	UMF	2729	1.05	427	187	0.16	2.30	2.46	0.07	15	2.34	0.53							
61	V-D	UMF	2851	1.01	431	117	0.14	1.18	1.32	0.11	14	1.31	0.60							
62	V-D	UMF	2872	1.16	428	428	0.29	1.83	2.12	0.14	25	1.83	0.54							
63	V-D	UMF	2876	1.02	431	137	0.19	1.40	1.59	0.12	19	1.56	0.60							
1	K-A	LMF	2496											20	50	30	0	30	0.61	
2	K-A	LMF	2570	0.84	441	244	0.68	2.05	2.73	0.25	81	3.25	0.78	30	20	50	0	50	0.58	
3	K-A	LMF	2596	0.46	441	106	0.04	0.65	0.69	0.06	9	1.50	0.78							
4	K-A	LMF	2669	1.50	443	261	0.38	3.92	4.30	0.09	25	2.87	0.81							
5	K-A	LMF	2750	0.62	438	162	0.11	1.01	1.12	0.10	18	1.81	0.72							
6	K-A	LMF	2786	0.36	442	20	0.06	0.47	0.53	0.11	17	1.47	0.80						0.65	
7	K-A	LMF	2792	0.44	445	72	0.02	0.26	0.28	0.07	5	0.64	0.85							
8	K-A	LMF	2972											30	10	50	10	60		
9	K-A	LMF	3156	0.46	444	81	0.06	0.36	0.42	0.14	13	0.91	0.83	30	10	50	10	60		
10	K-A	LMF	3224	0.29	444	58	0.04	0.17	0.21	0.19	14	0.72	0.83	20	10	50	20	70		
11	K-A	LMF	3316	0.73	448	76	0.09	0.35	0.44	0.20	12	0.60	0.90	20	10	50	20	70		

Table 2. (Continued).

				Organic geochemistry									Organic petrography							
SN	WName	Zone	Depth	TOC	Tmax	HI	S1	S2	GP	PI	OSI	RHP	VRcal	HOM	AOM	WOM	COM	W+C	%Ro	
12	K-B	LMF	2140	1.25	432	196	0.80	2.45	3.25	0.25	64	2.60	0.62							
13	K-B	LMF	2210	0.91	435	223	0.11	2.02	2.13	0.05	12	2.34	0.67	40	10	50	0	50	0.50	
14	K-B	LMF	2270	0.93	439	248	0.15	2.31	2.46	0.06	16	2.65	0.74							
15	K-B	LMF	2340	0.96	437	345	0.16	3.31	3.47	0.05	17	3.61	0.71							
16	K-B	LMF	2410	0.88	436	220	0.14	1.93	2.07	0.07	16	2.35	0.69	25	20	45	10	55	0.53	
17	K-B	LMF	2440	0.94	439	157	0.14	1.48	1.62	0.09	15	1.72	0.74							
18	K-B	LMF	2490	0.95	440	219	0.22	2.08	2.30	0.10	23	2.42	0.76							
19	U-C	LMF	2878	0.82	435	95	0.07	0.78	0.85	0.08	9	1.04	0.67							
20	U-C	LMF	3060											45	25	20	10	30	0.65	
21	U-C	LMF	3110	0.97	433	103	0.17	1.00	1.17	0.15	18	1.21	0.63							
22	U-C	LMF	3200											45	5	30	20	50	0.70	
23	U-C	LMF	3250	1.03	435	109	0.28	1.12	1.40	0.20	27	1.36	0.67							
24	U-C	LMF	3280	0.80	435	116	0.21	0.92	1.13	0.19	26	1.41	0.67							
25	U-C	LMF	3410											45	5	30	20	50	0.90	
26	V-D	LMF	2896	0.97	434	104	0.15	2.01	2.16	0.07	15	2.23	0.65	45	30	20	5	25	0.51	
27	V-D	LMF	2918	1.01	429	170	0.29	1.72	2.01	0.14	29	1.99	0.56							
28	V-D	LMF	3049	1.01	435	140	0.28	1.41	1.69	0.17	28	1.67	0.67							
29	V-D	LMF	3122	1.22	435	80	0.33	0.98	1.31	0.25	27	1.07	0.67							
30	V-D	LMF	3136	1.08	431	293	0.31	3.17	3.48	0.09	29	3.22	0.60	45	30	20	5	25	0.52	
31	V-D	LMF	3156	1.07	434	72	0.34	0.77	1.11	0.31	32	1.04	0.65							
32	V-D	LMF	3186	1.00	433	133	0.21	1.34	1.55	0.14	21	1.55	0.63							
33	V-D	LMF	3217	1.10	432	188	0.19	2.06	2.25	0.08	17	2.05	0.62							
34	V-D	LMF	3247	0.99	431	230	0.18	2.27	2.45	0.07	18	2.47	0.60							
35	V-D	LMF	3262	0.94	437	124	0.16	1.90	2.06	0.08	17	2.19	0.71							
36	V-D	LMF	3323	0.91	427	72	0.17	0.65	0.82	0.21	19	0.90	0.53							
37	V-D	LMF	3338	0.91	429	106	0.19	0.96	1.15	0.17	21	1.26	0.56							
38	V-D	LMF	3384	0.80	430	75	0.21	0.60	0.81	0.26	26	1.01	0.58							
39	V-D	LMF	3386	0.80	430	75	0.21	0.60	0.81	0.26	26	1.01	0.58	45	30	20	5	25	0.72	
40	V-D	LMF	3430	0.95	433	127	0.22	1.31	1.53	0.14	23	1.61	0.63							
41	V-D	LMF	3445	0.84	428	130	0.24	1.24	1.48	0.16	29	1.76	0.54							
42	V-D	LMF	3506	0.86	431	119	0.32	1.02	1.34	0.24	37	1.56	0.60							
43	V-D	LMF	3537	0.87	432	148	0.20	1.29	1.49	0.13	23	1.71	0.62							
44	V-D	LMF	3582	0.81	430	109	0.25	0.88	1.13	0.22	31	1.40	0.58							
45	V-D	LMF	3600											45	30	20	5	25	0.75	
46	V-D	LMF	3628	0.91	429	154	0.17	1.40	1.57	0.11	19	1.73	0.56							
47	V-D	LMF	3643	0.91	431	57	0.22	0.52	0.74	0.30	24	0.81	0.60							
48	V-D	LMF	3674	0.88	431	90	0.14	0.74	0.88	0.16	16	1.00	0.60							
49	V-D	LMF	3688	0.83	435	35	0.22	0.29	0.51	0.43	27	0.61	0.67	35	30	20	15	35	0.75	
50	V-D	LMF	3689	0.83	435	35	0.22	0.29	0.51	0.43	27	0.61	0.67							

UMF (UPPER MEZARDERE FORMATION)

Rock-Eval and maceral, vitrinite reflectance, palynological, and stable carbon isotope analyses. The first three analyses results are listed in Table 2. Selected age diagnostic dinocyst taxa identified in the palynological analyses are given in Figures 6a–6l and 7a–7l.

In our study, the liquid hydrocarbon contaminated samples were primarily dismissed by using the S1 vs. TOC plot shown in Figure 8 where absolute values of S1 over absolute values of TOC (S1/TOC ratio) greater than 100 show liquid contaminated samples. Hence, no sample having a S1/TOC > 100 is used. Secondly, mature–overmature samples were eliminated by using depth vs. Tmax, PI, and % Ro plots. Following mature sample elimination, new graphs are prepared and the results are given in Figures 9a–9c, where the samples are shown in two palynologically divided groups: Lower Mezardere Formation (LMF) and Upper Mezardere Formation (UMF), the details of which will be given in the following sections.

A total of 31 available palynological samples prepared using composite cutting samples of the Mezardere Formation penetrated in K-A, K-B, U-C, and V-D wells were analyzed. Palynological analyses of the 4 composite cutting samples in the K-A well (1902–1910 m, 2140–2148 m, 2206–2214 m, and 2348–2358 m) revealed an abundant and diverse dinocyst assemblage including *Wetzeliella symmetrica*, *Wetzeliella gochtii*, *Distatodinium ellipticum*, *Distatodinium craterum*, *Cordosphaeridium fibrospinosum*, *Homotryblium plectilum*, *Homotryblium pallidum*, *Batiacasphaera explanata*, *Polysphaeridium zoharyi*, *Spiniferites* spp., and *Hystrichokolpoma cinctum*. In addition to these dinocyst taxa, higher occurrences of *Pediastrum* spp. were observed in the 1902–1910 m sample. In the studied interval, all samples contain terrestrial palynomorphs, which are generally represented by conifers.

Palynological analysis of the Mezardere Formation in the K-B well yields a rich palynomorph assemblage having both terrestrial and marine taxa. The lower 5 samples (2080 m, 2222–2230 m, 2422–2430 m, 2638–2656 m, and 2828 m) have very abundant conifer taxa and dinocysts represented by *Homotryblium plectilum*, *Cordosphaeridium* sp., *Distatodinium ellipticum*, *Operculodinium* sp., *Cleistosphaeridium placacanthum*, *Cleistosphaeridium*

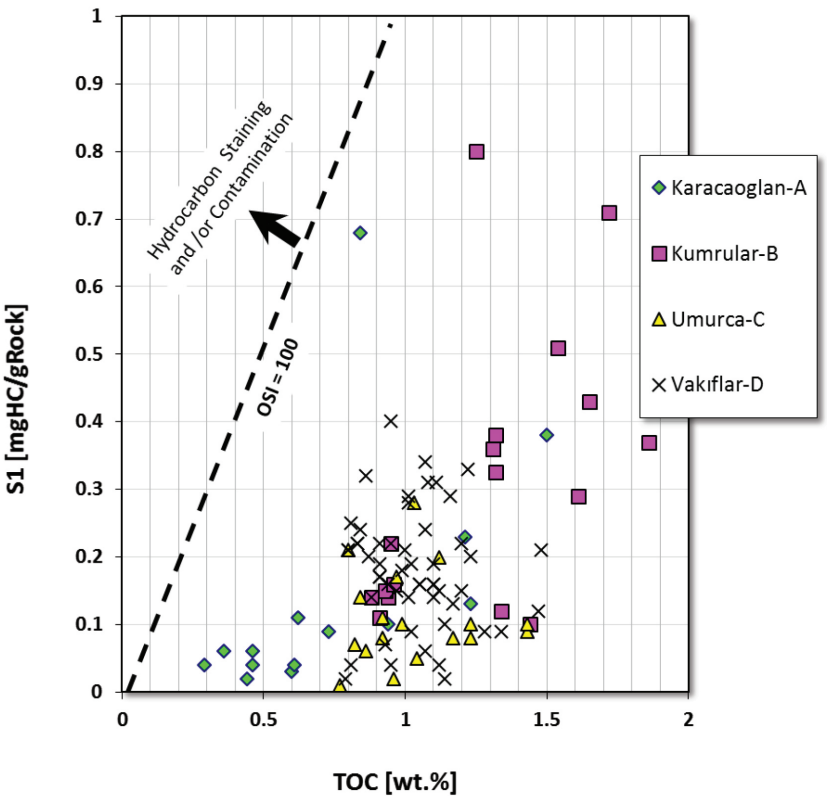

Figure 8. TOC vs. S1 plot showing possible contamination of the Mezardere Formation samples by liquid hydrocarbons. This figure indicates that the Mezardere samples used in this study are not significantly contaminated by migrated hydrocarbons. Note that "OSI > 100" shows contaminated samples. OSI = oil saturation index = (S1/TOC) × 100 (Jarvie et al., 2001). Localities of the studied wells are given in Figure 4.

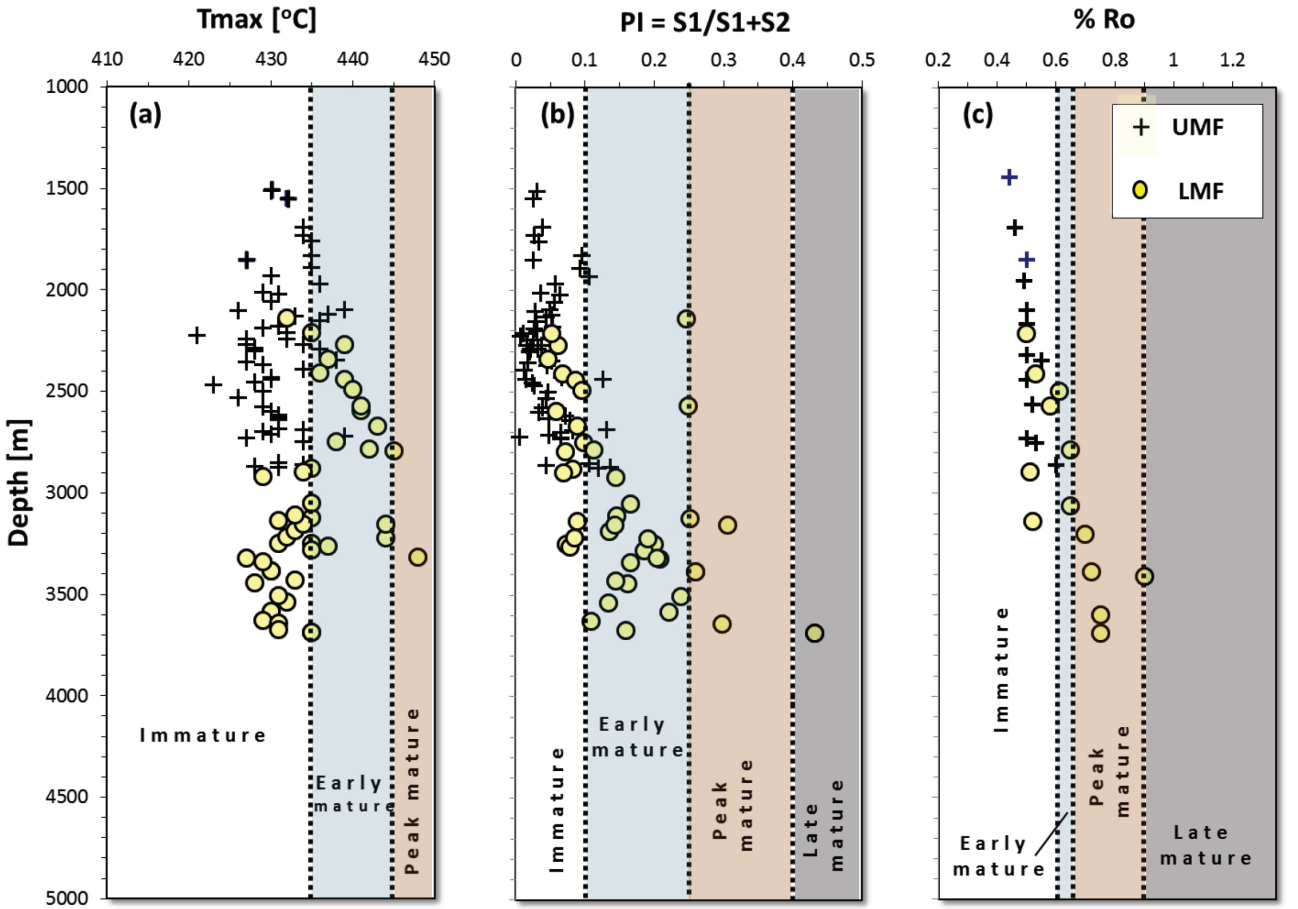

Figure 9. Geochemical logs of Tmax (a), PI (production index) (b), and % Ro (c) indicating that most of the Mezardere Formation samples are immature to early mature. However, four samples are peak mature and one sample appears to be late mature. Note that there are some maturity variations among different maturity parameters.

ancyreum, *Spiniferites* spp., *Distatodinium ellipticum*, *Operculodinium centrocarpum*, and *Glaphyrocysta* cf. *semitecta.* A few *Wetzeliella* specimens very close to *Wetzeliella gochtii* and/or *Wetzeliella ovalis* were also encountered in these lower samples representing the lower part of the Mezardere Formation. Stratigraphically higher 5 samples (1400–1408 m, 1590–1598 m, 1732–1740 m, 1900–1908 m, and 1960 m) yielded abundant occurrences of a diverse dinocyst assemblage characterized by *Wetzeliella gochtii*, *Homotryblium plectilum*, *Rotnestia borussica*, *Hystrichokolpoma cinctum*, *Homotryblium abbreviatum*, *Cleistosphaeridium placacanthum*, *Cleistosphaeridium ancyreum*, *Chiropteridium* sp., *Spiniferites* spp., *Distatodinium ellipticum*, and *Operculodinium centrocarpum*. In addition to those dinocysts, *Pediastrum* spp. have higher occurrences in 1590–1598 and 1960 m samples. Terrestrial pollen grains represented mostly by conifers are very rich in 1400–1408 m and 1732–1740 m samples.

Eight samples (2150–2170 m, 2320–2340 m, 2560–2570 m, 2750–2760 m, 2860 m, 3060 m, 3200 m, and 3410–3420 m) were investigated in the U-C well. Relatively poor to moderate occurrences of palynomorph taxa were identified in these samples. Three stratigraphically lower samples (3060–3420 m interval) are represented by higher occurrences of terrestrial taxa (mostly conifers) and very rare occurrences of dinocysts. *Pediastrum* spp. have abundant occurrences at 3200 m. The 5 stratigraphically higher samples (2150–2860 m interval) rich in amorphous organic matter are characterized by higher occurrence of *Wetzeliella gochtii* (e.g., 2860 m sample) and sporadoic occurrences of *Batiacasphaera explanata*, *Tenua hystrix*, *Impagidinium* sp., and *Homotryblium plectilum*. Terrestrial palynomorphs are represented mostly by conifers. *Pediastrum* specimens are very abundant in the 2860 m sample.

Finally, the Mezardere Formation penetrated in the V-D well is palynologically analyzed in 9 samples (1892–

1904 m, 2116–2156 m, 2326–2334 m, 2618–2658 m, 2724–2744 m, 2874–2886 m, 3136–3152 m, 3300–3350 m, and 3688–3700 m). The palynomorph assemblage of the samples is very close to that of the K-B well. Two different assemblages characterize the Mezardere Formation. The first assemblage identified in the lower part of the Mezardere Formation (3136–3700 m interval) is characterized by very rich terrestrial palynomorphs and lower occurrences of dinocysts represented by *Deflandrea* sp., *Cleistosphaeridium* spp., *Cordosphaeridium fibrospinosum*, *Tenua hystrix*, *Glaphyrocysta* cf. *semitecta*, and *Batiacasphaera explanata*. Five of the 6 stratigraphically higher samples (1892–2886 m interval) have a very rich and diverse dinocyst assemblage represented by *Wetzeliella ovalis*, *Wetzeliella gochtii*, *Diphyes colligerum*, *Tenua hystrix*, *Distatodinium ellipticum*, *Distatodinium craterum*, *Homotryblium plectilum*, *Cleistosphaeridium* spp., and *Lejeunecysta* sp. Higher occurrences of *Pediastrum* spp. and terrestrial palynomorphs (*Pinus*, Taxodiaceae, *Ulmus*, *Alnus*, *Carya*, and fungal spores) are observed in 2116–2156 m, 2618–2658 m, and 2724–2744 m samples, respectively.

5. Discussion

5.1. Subdivision of the Mezardere Formation based on dinocyst biostratigraphy

Based on the palynological data given in the results, considering two different dinocyst assemblages, the Mezardere Formation was informally subdivided into two as the Lower Mezardere Formation (LMF) and Upper Mezardere Formation (UMF). The dinocyst assemblage in the LMF (corresponding to 2080–2828 m, 3060–3420, and 3136–3700 mm intervals in K-B, U-C, and V-D wells, respectively) includes long ranging *Homotryblium* spp., *Cordosphaeridium* sp., *Distatodinium* spp., *Operculodinium* spp., *Cleistosphaeridium* spp., and *Spiniferites* spp. Single to rare occurrences of age-diagnostic *Glaphyrocysta* cf. *semitecta* specimens in the LMF are remarkable. On the other hand, the UMF (corresponding to 1902–2358 m, 1400–1960 m, 2150–2860 m, and 1892–2886 m intervals in K-A, K-B, U-C, and V-D wells, respectively) comprises predominantly long-ranging cosmopolitan taxa with very limited biostratigraphic value, such as *Spiniferites* spp., *Operculodinium* spp., *Distatodinium* spp., *Homotryblium* spp., and *Cleistosphaeridium* spp. However, a number of age-diagnostic Wetzellielloid taxa (notably *Wetzeliella gochtii* and *Wetzeliella symmetrica*) are also present in the samples belonging to these given intervals. *Glaphyrocysta* cf. *semitecta* is an important age diagnostic dinocyst for the LMF in the studied well sections having a stratigraphic distribution covering NP21 and NP22 zones of the Early Oligocene in the Mediterranean and Northern Europe (Wilpshaar et al., 1996; Torricelli and Biffi, 2001; Williams et al., 2004; Van Simaeys et al., 2005; Pross et al., 2010; Bati, 2015). For the UMF, *Wetzeliella gochtii* is a very important biostratigraphic tool having a particular importance for the regional correlations and being one of the stratigraphic markers for the Oligocene, where its first occurrence (FO) is commonly used to recognize the Early Oligocene. There are many studies reporting the Early Oligocene FO of this taxon (e.g., Costa and Downie, 1976; Liengjarern et al., 1980; Köthe, 1990; Powell, 1992; Brinkhuis and Biffi, 1993; Bati et al., 1993; Williams et al., 2004; Gradstein et al., 2004; Gedl, 2004; Eldrett et al., 2004; Dybkær, 2004; Van Simaeys et al., 2005; Sancay, 2005; Sancay et al., 2006a, 2006b; Köthe and Piesker, 2007; Bati and Sancay, 2007; Bati et al., 2007; Pross et al., 2010; Barski and Bojanowski, 2010; Soliman, 2012; Bechtel et al., 2013, 2014; Bati, 2015; Sachsenhofer et al., 2017). However, Pross (2001) and Sluijs et al. (2005) suggested that the last occurrence (LO) of Wetzellioid dinoflagellate cysts including *Wetzeliella symmetrica* and *Wetzeliella gochtii* reflects strong diachronism in that younger LOs occurred in the northwest European Tertiary Basin. Older LOs, with a 3.6 m.y. time difference, occurred in the southern part of Europe, because of the seaway connection between the Tethys and northwest European Basin. Nevertheless, the LO of *Wetzeliella gochtii* is generally accepted to fall within the Early Chattian (e.g., Van Simaeys et al., 2005; Coccioni et al., 2008; Sachsenhofer et al., 2010; Bechtel et al., 2014). Based on these findings, its magnetostratigraphically calibrated range extends from the Early Rupelian (33.1 Ma) to the Early Chattian (26.4 Ma) (Pross et al., 2010) corresponding to nannofossil zones NP22–NP25. Similarly, the first and last occurrences of *Wetzeliella symmetrica* are reported as earliest Rupelian and Chattian (Köthe, 1990; Powell, 1992; Pross et al., 2010; Bechtel et al., 2014).

The last decade of the second millennium was the period during which several biostratigraphic studies based on dinocysts were carried out to establish well-calibrated dinoflagellate cyst zonal schemes in different regions of the Mediterranean and Eastern Europe (Bati, 2015 and references therein). As one of the pioneering works, Brinkhuis and Biffi (1993) defined eight dinoflagellate cyst zones (*Melitasphaeridium pseudorecurvatum* (Mps), *Schematophora speciosa* (Ssp), and *Cordosphaeridium funiculatum* (Cfu) interval zones in the Upper Eocene; *Achomosphaera alcicornu* (Aal) Interval zone in the Eocene–Oligocene transition; and the *Glaphyrocysta semitecta* (Gse), *Areosphaeridium diktyoplokum* (Adi), *Reticulatosphaera actinocoronata* (Rac), and *Corrudinium incompositum* (Cin) interval zones in the Lower Oligocene) on the basis of 20 dinocyst events they described. Later, Wilpshaar et al. (1996) studied Oligocene dinoflagellate cysts in samples from Central Italy. They integrated their new data with the previously established Lower and

uppermost Oligocene zonations (Brinkhuis and Biffi, 1993) and presented a formal dinocyst zonation that encompassed eleven interval zones with two new Oligocene dinocyst zones proposed (*Hystrichokolpoma pusillum* and *Chiropteridium lobospinosum* interval zones) spanning the entire Oligocene. Among these studies, Brinkhuis and Biffi (1993) and Pross et al. (2010) stated that *Wetzeliella gochtii* occurred for the first time in their *Reticulatosphaera actinocoronata* (Rac) Interval Zone, equivalent to the middle part of the calcareous nannoplankton zone NP21 interpreted as early Early Oligocene in age in Italy. There are many other works in which the FO of *Wetzeliella gochtii* is given in *Reticulatosphaera actinocoronata* (Rac) Interval Zone (Wilpshaar et al., 1996; Torricelli and Biffi, 2001; Pross et al., 2010; Bati, 2015). Powell (1992) indicated that the first occurrence datum of *Wetzeliella gochtii* marked the base of the dinocyst biozone Wgo (Lower Rupelian), which corresponded to the base of calcareous nannofossil Biozone NP22. The same event was detected by Eldrett et al. (2004) and van Simaeys et al. (2005) in the Norwegian–Greenland Sea and North Sea basins, respectively. Zaporozhets (1999) in his palynostratigraphic work covering Middle Eocene–Lower Miocene deposits in the Belaya River area (Northern Caucasus) defined 9 dinocyst zones and reported that the *Wetzeliella gochtii* zone corresponded to NP23. Later, Sachsenhofer et al. (2017), in their Oligocene–Lower Miocene study in the same area, defined the *Wetzeliella gochtii* zone in the Polbian ("Ostracoda") Bed corresponding to the NP23 zone as well. Regarding the Turkish occurrences of *Wetzeliella gochtii*, it was recorded in the Thrace Basin corresponding to the Rupelian-aged *Wetzeliella gochtii–Distatodinium ellipticum* zone defined by Bati et al. (1993, 2007) and Turgut and Eseller (2000), and in the middle part of the Rupelian, corresponding to NP23-24 within the P-Rp1 zone of Bati and Sancay (2007) defined for the first time in Eastern Anatolian Oligocene units.

Based on the paleogeographic position of the Thrace Basin during the Early Oligocene deposition of the Mezardere Formation and the Eastern Paratethys zonal schemes, a ?Pshekian age corresponding to NP 21/22 zones can be assigned for the LMF based on the presence of *Glaphyrocysta* cf. *semitecta* in some samples of the K-B and V-D wells. Similarly, a Solenovian age corresponding to NP23/24 zones based on the first and last occurrences of *Wetzeliella gochtii* is assigned for the UMF. Absence of *Areosphaeridium diktyoplokum*, *Thallasiphora pelagica*, *Achomosphaera alcicornu*, *Phthanoperidinium* spp., *Cordosphaeridium funiculatum*, *Distatodinium biffii*, *Chiropteridium*-abundance, *Deflandrea*-abundance, and *Caligodinium pychnum* in the LMF and UMF support this age assignment.

5.2. Paleodepositional environment of the Mezardere Formation

Concerning the depositional setting of the Mezardere Formation, the overall palynomorph assemblage having higher terrestrial palynomorphs in the LMF samples may indicate shallower neritic conditions during the ?Pshekian. On the other hand, the dinocyst-rich assemblage having abundant *Wetzeliella gochtii* specimens encountered in the UMF reflects a neritic environment during the Solenovian. This interpretation is based on the data from Sluijs et al. (2005) and Pross and Brinkhuis (2005) giving the systematic model for the distribution of dinocyst associations during the Paleogene. In their work, Sluijs et al. (2005) and Pross and Brinkhuis (2005) used presence/dominance of *Homotryblium* spp., *Wetzeliella* spp., *Operculodinium* sp., *Spiniferites* spp., and *Cleistosphaeridium* spp. to signify nutrient-rich surface waters/near shore environment. Similar observations, based on the presence/dominance of the same taxa, were made by Sachsenhofer et al. (2010) for the depositional history of the Oligocene Eggerding Formation, in the Molasse Basin of Austria, which was a part of the Central–Western Paratethys; by Gedl (2004) in Šambron beds in the Central Carpathian Palaeogene, in Slovak Orova; by Sachsenhofer et al. (2015) for the deposition of Early Oligocene-aged Bituminous Marl Member; and by Schulz et al. (2004, 2005) for the deposition of the Early Oligocene (Kiscellian) Schöneck Formation, Dynow Marlstone, and Eggerding Formation in the Austrian Molasse Basin. Schulz et al. (2004, 2005) specified that the high primary production level during the deposition of the Dynow Marlstone promoted cyclic blooms of calcareous nannoplankton under brackish surface water. Similarly, Bechtel et al. (2012) in their work in the Lower Oligocene Tard Clay of Hungary specified that the upper part of the Tard Clay was deposited during the Kiscellian (corresponding to calcareous nannoplankton zone NP23) under heavy fresh water influx, which promoted richness in nutrients and high bioproductivity. Schulz et al. (2005) related these nannoplankton blooms to the restriction of the surface inflow of salty water during NP23, with ongoing narrowing of the seaways in the Western Paratethys, with massive freshwater runoff spread as surface flows.

The studied UMF samples in the K-A well (1902–1910 m), in the K-B well (1590–1598 and 1960 m), in the U-C well (2860 m), and in the V-D well (2116–2156 m, 2618–2658 m, and 2724–2744 m) have higher occurrences of green algae *Pediastrum* spp. even in dinocyst-rich samples. In some of these samples *Pediastrum* spp. and *Wetzeliella gochtii* have been identified abundantly. *Pediastrum* spp. is accepted to represent fresh water (Ediger and Bati, 1988 and references therein) and estuarine/brackish environments (Sachsenhofer et al., 2010). On the other hand, Wetzelielloid dinocysts are accepted to represent lagoonal, estuarine, shelf, or brackish water environments tolerating reduced

salinity (Jaramillo and Oboh-Ikuenobe, 1999). Higher abundances of *Pediastrum* spp. in the UMF samples with marine dinocysts (e.g., *Wetzeliella gochtii*) may indicate brackish water settings during some parts of the depositional history of the UMF in the Solenovian, which may correspond to heavy fresh water influx promoted richness in nutrients and nannoplankton blooms as mentioned by Schulz et al. (2004, 2005) and Bechtel et al. (2012) in the Paratethys area. Presence of *Pediastrum* specimens in the 3200 m sample of the LMF in the U-C well may specify similar conditions in the ?Pshekian, as well.

5.3. Application of geochemical proxies for potential sea level fluctuation indicator

Aside from source rock petroleum potential studies, recent studies show that some of the Rock-Eval parameters can be also used as potential proxies for sea level fluctuations. Furthermore, the particularly vertical distribution of the TOC and HI and more recently introduced parameter RHP (S1+S2/TOC) have been used as potential proxies for sea level fluctuations (Habib and Miller, 1989; Pasley and Hazel, 1990; Pasley et al., 1991; Creaney and Passey, 1993; Hart et al., 1994; Slatt and Rodriguez, 2012; Freire and Monteiro, 2013; Song et al., 2014).

Habib and Miller (1989) noted that changes in kerogen type could be a useful indicator in delineating transgressive and regressive intervals. More importantly, less terrestrially derived organic matter is present in transgressive sequences and, conversely, maceral facies in regressive sediments contain more terrestrially derived woody and coaly OM. Hart et al. (1994) claimed that during transgression of the shoreline terrigeneous sediment is deposited in estuarine and coastal environments, and consequently little is introduced to the shelf in the San Juan Basin of New Mexico and Colorado. Hart et al. (1994) interpreted that the Upper Cretaceous Lower Mancos Shale in the Piceance Basin, USA, represents deposits of a sea level regression and Upper Mancos Shale represents deposits of a sea level transgression. They realized two differences between the two. Transgressive Upper Mancos Shale has lower terrestrial OM %, higher HI, and higher TOC than those from the regressive Lower Mancos Shale. Similar work by Hart et al. (1994) was applied to the modern depositional environments by Omura and Hoyanagi (2004), who reported that during transgression terrestrial organic matter is trapped in estuarine environments of the shelf. Freire and Monteiro (2013) used an organic geochemical proxy called the "TOMI Index" for the recent sediments of the Japan Sea to determine sea level changes. The TOMI index is derived from the $\delta^{13}C$ values of kerogen combined with the TOC to total nitrogen ratio of the organic matter in the recent sediments.

The RHP, which is used in this study as a potential sea level fluctuation indicator, is derived from Rock-Eval pyrolysis S1, S2, and TOC as formulated RHP = (S1 + S2)/TOC (Table 2). As seen from the formula, RHP covers S1, TOC and HI (S2 × 100/TOC. This parameter was first used by Fang et al. (1993), who applied it to Chinese lacustrine shales. Based on the RHP, Fang et al. (1993) established two main vertical organic facies sequences (VOFS): "rising-upward (sea level) sequence" and "falling-upward sequence". A rising-upward VOFS represents a change in organic facies from hydrogen poor to hydrogen rich from the base to top of the stratigraphic sequence. This, in turn, indicates a change from oxic to anoxic conditions "sea level rising" and in turn indicates better preservation of organic matter. In contrast, a falling-upward VOFS represents an upward vertical change in organic facies from hydrogen rich to hydrogen poor, corresponding to a change from anoxic to oxic conditions "sea level falling", where less organic matter is preserved.

An applicability of the RHP as an indicator of sea level variation along the four wells studied is tested in Figures 10a–10d. Detailed examination of the curves along the four wells resulted in identification of 3 full or partial, short-term transgressive–regressive cycles in each well within an overall transgression (Turgut and Eseller, 2000). The transgressive and regressive parts of each cycle vary in thickness depending, in part, on whether a complete cycle is present. Interestingly enough, the Solenovian UMF in the K-A, K-B, U-C, and V-D wells corresponds to Cycle 3, Cycle 2+3, Cycle 2+3, and Cycle 2+3, respectively. Among these, it appears that the K-A well acts partly independently (Figure 10a). Variations in the TOC, HI, and RHP values along the depth of the K-A, K-B, U-C, and V-D wells are shown in Figures 11–14, respectively. These figures also support the conclusion that there is a third-order transgression from ?Pshekian to Solenovian as indicated by a large arrow in Figures 11–14. The significance of these diagrams is that they give a signal of the organic-rich intervals. In our case both organic- and HI-rich intervals took place in the UMF zone corresponding to the upper portion of the third-order transgression, which may be called a highstand systems tract (HST) in the sequence stratigraphy terminology.

AOM % vs. depth and (W+C) % vs. depth plots on the basis of LMF and UMF samples are shown in Figures 15a and 15b. As a first sign, one may notice that AOM % increases with decreasing depth (Figure 15a), whereas (W+C) % decreases with decreasing depth (Figure 15b). This is what we expect if the samples of the LMF zone belong to a regressive sequence, whereas those of the UMF zone belong to a transgressive sequence. Consequently, this finding can be thought as additional evidence of increasing intensity of transgression from the ?Pshekian to Solenovian along the wells that penetrated the MF.

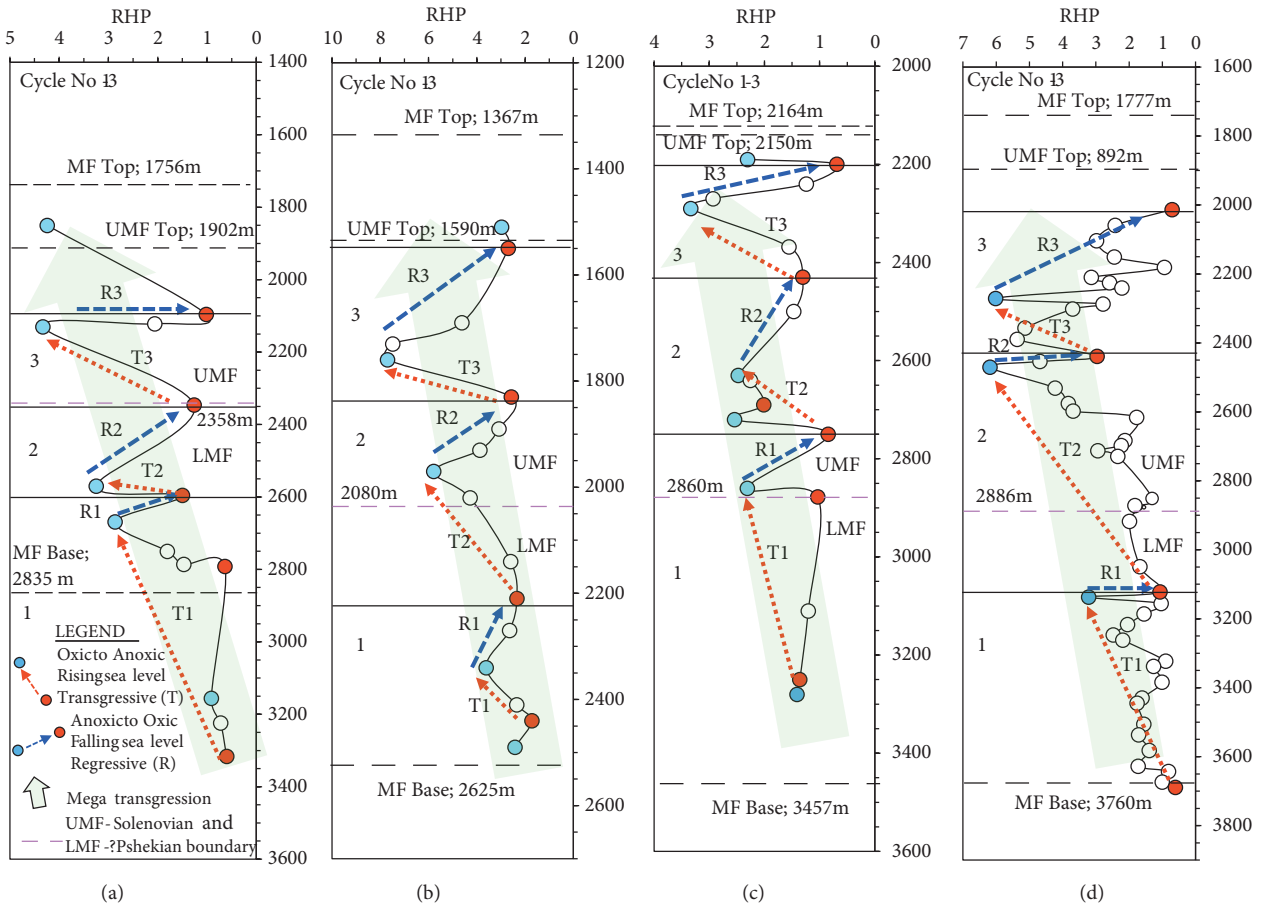

Figure 10. Sea level fluctuations on the basis of relative hydrocarbon potential (RHP) logs of the four wells studied: (a) K-A well, (b) K-B well, (c) U-C well, and (d) V-D well. Note the increasing RHP values (i.e. increasing anoxicity) of the Lower Oligocene Mezardere samples from base to top, implying the occurrence of a sea level rise or transgression. Also note that smaller transgressive/regressive cycles are superimposed on the overall sea level rise. Well abbreviations and locations are given in Figure 4.

5.4. Source rock evaluation

5.4.1. Source rock potential

The samples used in the analyses are selected regardless of the unfavorable visual appearance of the samples (i.e. lack of black color) with respect to high OM. Therefore, source rock and petroleum potential of the MF is evaluated based on not only the deliberately selected samples with probably high organic richness but also the samples with poor organic richness considered. Source rock and petroleum potential assessment of the MF that is fully penetrated in the studied four wells is evaluated considering two zones as proposed and depicted in the earlier sections: LMF and UMF. Descriptive statistics of average organic geochemical and organic petrographical parameters derived from both zones are given in Tables 3a and 3b.

Organic richness

LMF: Organic richness of the rock samples is measured as TOC. TOC values of 0–0.5, 0.5–1.00, 1.00–2.00, and >2.00 wt. % indicate poor, fair, good, and very good source rock character, respectively (Peters, 1986). The TOC values of the LMF range from 0.29 to 1.50 wt. % with an average value of 0.88 wt. % (Table 3a; Figure 16). S2 yield, on the other hand, ranges from 0.17 to 3.92 mg HC/g rock and averages at 1.32 mg HC/g rock, indicating that the LMF has a poor petroleum potential. It should be kept in mind that the samples selected from the LMF and the UMF zones are early to marginally mature; therefore, thermal maturation cannot be responsible for the lower TOC and S2 yields. The PCC between TOC and S2 of the LMF samples is 0.66 (Table 4).

UMF: The TOC values of the UMF samples range from 0.60 to 1.86 wt. % with an average of 1.15 wt. % (Table 3b). Accordingly, the UMF is considered a good source rock if only TOC is considered.

The TOC is an important criterion for source rock evaluation; however, it must not be used alone. Parameters

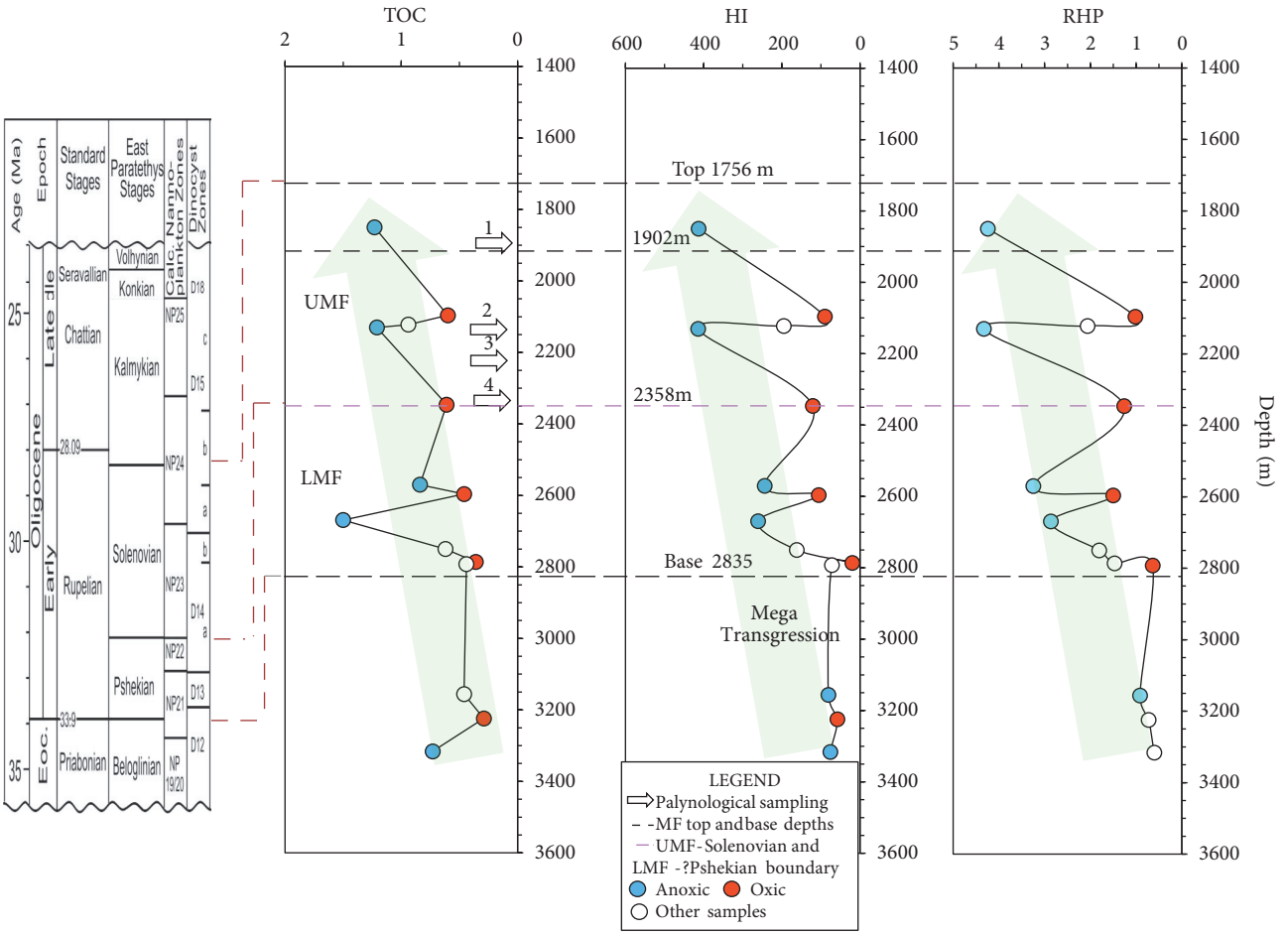

Figure 11. TOC, HI, and RHP logs of the K-A well. Informal subdivision of the Mezardere Formation into the Lower Mezardere Formation (LMF) and the Upper Mezardere Formation (UMF) on the basis of dinocyst assemblages and *Pediastrum* spp. (see text) is compatible with the organic geochemical TOC, HI, and RHP log curves. Legend in this figure is applicable to Figures 12–14. Location of the well is given in Figure 4.

such as S2 yield are almost compulsory to use with TOC. Assessment of TOC and S2 values must be realized on the immature–marginally mature rock samples as done in this study. If TOC and S2 yield values are 0.0–0.5 wt. % and 0–2.5 mg HC/g rock, then the analyzed rock sample has a poor potential; 0.5–1.0 wt. % and 2.5–5 mg HC/g rock, it has a fair potential; 1.0–2.0 wt. % and 5–10 mg HC/g rock, it shows a good potential; and lastly 2.0–4.0 wt. % and 10–20 mg HC/g rock, it is a very good potential source rock (Tissot and Welte, 1984; Peters, 1986; Peters and Cassa, 1994). Therefore, we should examine an internal relation between TOC and S2 yield. Figure 17 shows a TOC vs. frequency histogram of the UMF samples grouped by S2 yield. For example, the bar showing highest frequency (13) shows a TOC value of 1.00–1.25 wt. %, which indicates a good source rock (Peters, 1986), but S2 yield of the same bar is 0.0–2.5 mg HC/g rock, which indicates a poor potential (Figure 17). Hence, the relatively high TOC (1.00–1.25 wt. %) value of a rock sample is needed to be evaluated together with S2 yield. However, S2 yield alone is a much better indicator of organic richness. In fact, its range for the UMF samples changes from 0.54 to 13.55 mg HC/g rock and averages at 3.52 mg HC/g rock, indicating that the UMF has a fair petroleum potential (see discussion above). The PCC between TOC and S2 within the UMF samples is 0.76 (Table 5).

Organic matter type

Organic matter type present in the rock is important to determine the type of the ultimately generated hydrocarbons. Lacustrine/marine type I OM with HI (mg HC/g TOC) values > 600 yields mostly oil, marine type II OM with HI = 300–600 yields oil, mixed type II/III OM with HI = 200–300 yields oil and gas, continental type III OM with HI = 50–200 yields gas, and lastly degraded type

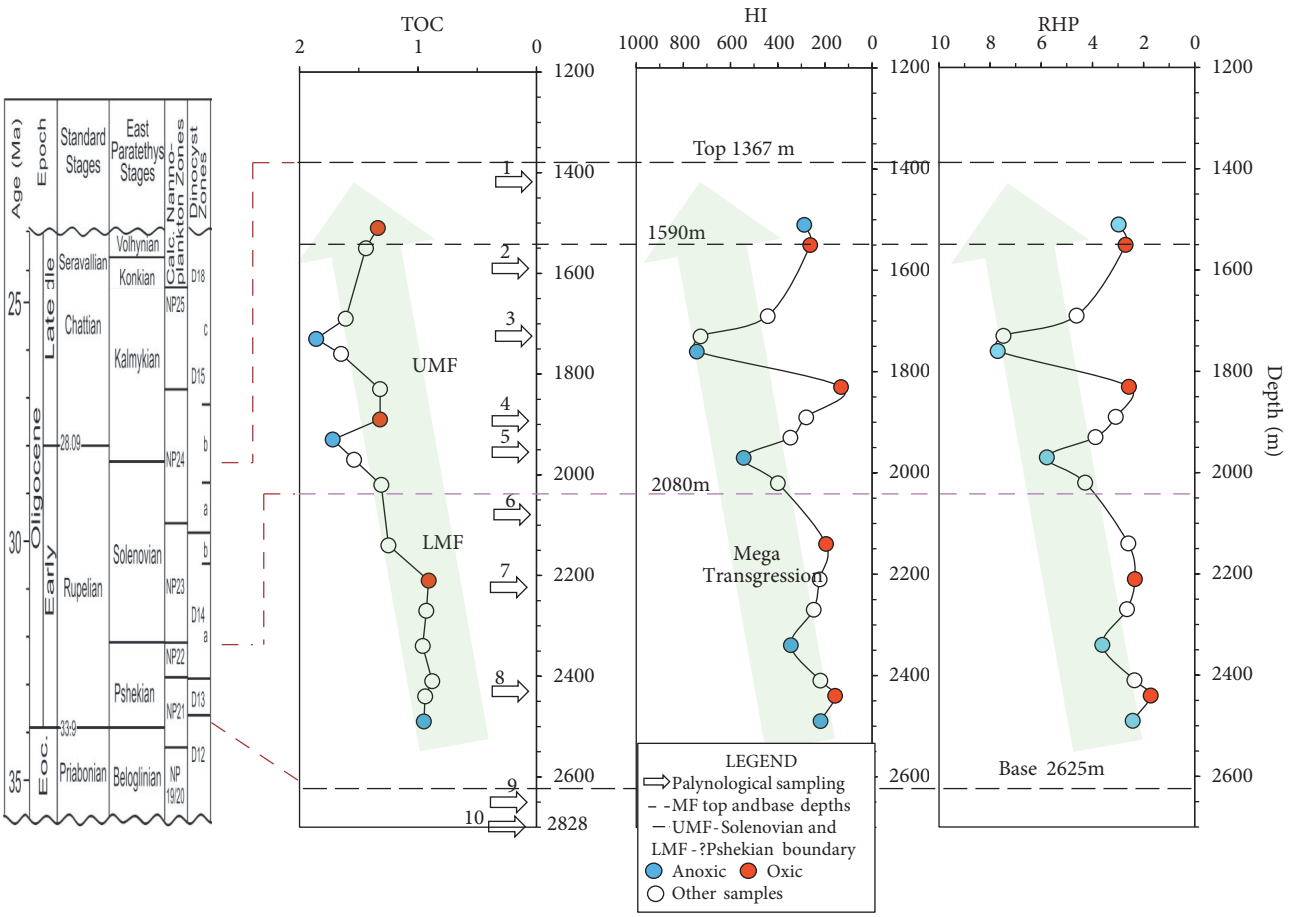

Figure 12. TOC, HI, and RHP logs of the K-B well. Informal subdivision of the Mezardere Formation into the Lower Mezardere Formation (LMF) and the Upper Mezardere Formation (UMF) on the basis of dinocyst assemblages and *Pediastrum* spp. (see text) is compatible with the organic geochemical TOC, HI, and RHP log curves. Location of the well is given in Figure 4.

IV OM with HI < 50 yields no oil or gas (Peters and Cassa, 1994). Type IV OM is inert and contains little hydrogen, and has no hydrocarbon-generating capacity. The other approach to determine organic matter type in this study is microscopic study on the kerogen slides to get percent maceral types.

LMF: The HI values of the LMF samples have a minimum at 20 and maximum at 345 and average at 136 mg HC/g TOC (Table 3a). If we consider the average value of 136 mg HC/g TOC alone, gas prone type III OM is the major OM type in the LMF samples. The Tmax versus HI diagram is also used to define organic matter types in the rock samples (Figure 18). In this figure, the samples remain constantly on the Tmax = 430–435 °C maturation curve (i.e. % Ro = 0.58–0.60 curve), indicating that HI is mainly affected by the input of organic matter type into the depositional environment, and in turn affected by fluctuations in sea level (Figure 18). Accordingly, HI in the LMF samples shows a great range indicating mixed type II/III, type III, and type IV organic matter. This organic type basically implies a shallow-coastal marine environment (i.e. neritic) receiving various type continental organic matter from the land. Analysis of the LMF kerogen slides is performed to provide the maceral % distribution in the MF samples. The mean values from the most abundant to less abundant maceral type % for the LMF samples are follows: WOM % = 35, HOM % = 35, AOM % = 20, and COM % = 10 (Table 3a; Figure 19a). This result is consistent with the HI data given in Table 2. Within the 17 parameters given in Table 2, the highest and negative PCC is found between the COM % and HI (r = –0.66; Table 4).

UMF: The HI values of the UMF samples have a minimum at 67 and maximum at 744 and average at 285 mg HC/g TOC (Table 3b). Considering the average value of 285 mg HC/g TOC alone, we can say that mixed type II/III kerogen is the major OM type in this zone. Similar to the LMF samples, the UMF samples remain constantly

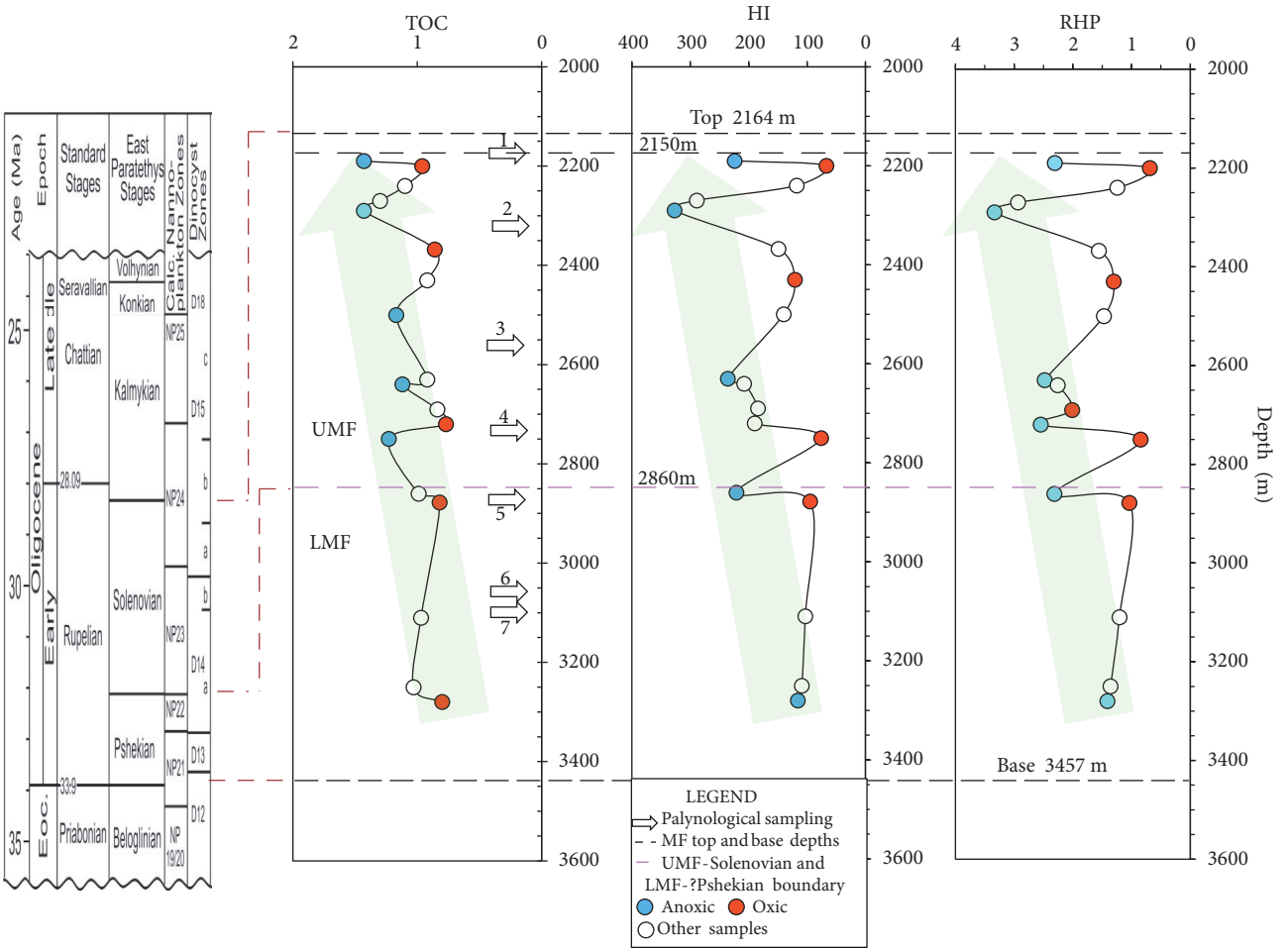

Figure 13. TOC, HI, and RHP logs of the U-C well. Informal subdivision of the Mezardere Formation into the Lower Mezardere Formation (LMF) and the Upper Mezardere Formation (UMF) on the basis of dinocyst assemblages and *Pediastrum* spp. (see text) is compatible with the organic geochemical TOC, HI, and RHP log curves. Location of the well is given in Figure 4.

on the Tmax = 430–435 °C maturation curve (i.e. % Ro = 0.58–0.60 curve), indicating that HI is mainly affected by the input of organic matter type and sea level fluctuations in the depositional environment having input of type I, type II, and mixed type II/III organic matter (Figure 18). Input of type I OM is supported by the existence of *Pediastrum* spp. in the UMF samples. Organic matter type assessment under the microscope suggests that the UMF samples show mean values as AOM % = 37, HOM = 29, WOM % = 28, and COM % = 6 on average (Table 3b; Figure 19b). The highest Pearson correlation occurs between the AOM and HI (r = 0.41; Table 5).

On average, the organic matter type of the ?Pshekian LMF samples can be classified as type III kerogen, whereas the organic matter type of the Solenovian UMF samples is composed of type II/III kerogen. These results again support the findings of our study that the LMF consists of predominantly regressive continental OM-rich deposits, whereas the UMF consists of marine OM-rich transgressive deposits.

Thermal maturity

In the present study, in order to remove the thermal maturation effect on the geochemical sea level proxies of TOC, HI, and RHP, the mature–postmature MF samples were eliminated. As a result, only early mature or marginally mature samples were used in this study (see Figures 9a–9c). Therefore, there is no further need for evaluation of the thermal maturity of the MF samples (Figure 18). Furthermore, it is interesting to note that in Figures 9b and 9c two of the maturity parameters, namely PI = S1/S1+S2 and % Ro, show regular increase with depth, whereas the other thermal maturity parameter, Tmax, decreases irregularly after about 2900 m. This is a common phenomenon in the Thrace Basin since oil generation begins at about 2900–3000 m in the basin (Gürgey, 2015). Therefore, the samples we analyzed contain some of the

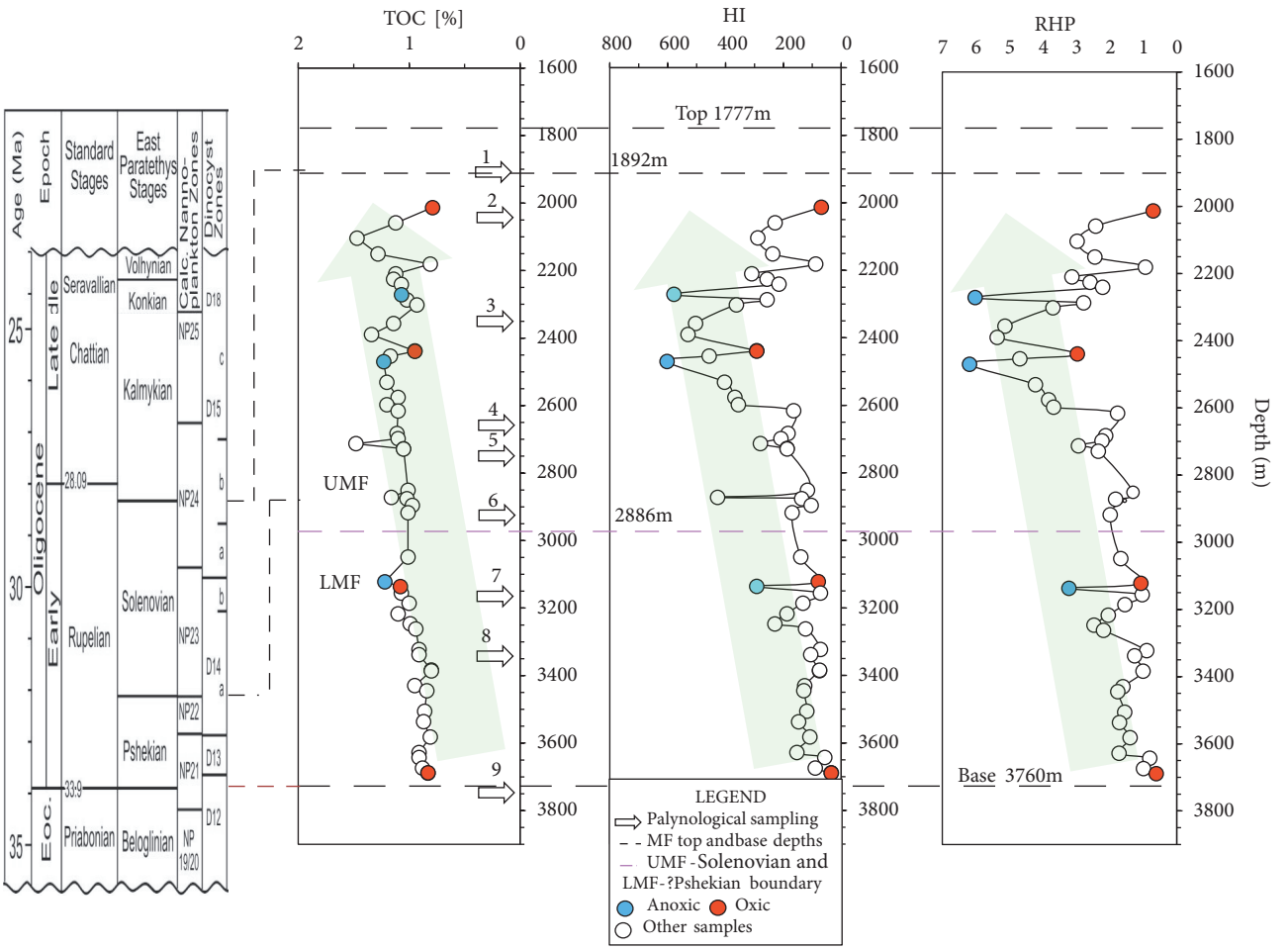

Figure 14. TOC, HI, and RHP logs of the V-D well. Informal subdivision of the Mezardere Formation into the Upper Mezardere Formation (UMF) and Lower Mezardere Formation (LMF) based on the dinocyst assemblages and *Pediastrum* spp. (see text) is compatible with the organic geochemical TOC, HI, and RHP log curves. Location of the well is given in Figure 4.

generated hydrocarbons that cause decreasing Tmax values measured by the Rock-Eval Pyrolsis device.

5.4.2. Petroleum potential

The petroleum potential of the rock samples is usually evaluated by using Rock-Eval pyrolysis parameters, such as S1, S2, and genetic potential (GP = S1 + S2 mgHC/g rock; Tissot and Welte (1984). GP < 2, TOC = 0–0.5; GP = 2–6, TOC = 0.5–1; GP > 6, TOC = 1–2; and GP > 6, TOC > 2 indicate poor, fair, good, and excellent petroleum potential, respectively. Hence, the GP vs. TOC plot seems to be a useful way of evaluating petroleum potential (Figure 20). As seen in this figure, fair–good to excellent petroleum potential of the UMF samples is remarkable. In contrast, most of the LMF samples show poor to fair petroleum potential except for seven samples, which show fair petroleum potential. It should be remembered that the LMF samples are considered to represent the regressive deposits, which in general, show low TOC and HI; consequently, their low petroleum potential of the LMF samples then inevitably occurs. Petroleum potential of the MF samples is also assessed by using the source potential index (SPI). The SPI gives an estimate of the initial petroleum potential of a source rock. SPI is calculated using the formula:

SPI = h × (S1 + S2) × ρ/1000, (Demaison and Huizinga, 1991)

where

SPI = ton HC/m^2 = t HC/m^2

h = Source rock thickness (m);

S1 = Average Rock-Eval S1 (kg HC/tons of rock);

S2 = Average Rock-Eval S2 (kg HC/ ton of rock); and

ρ = Density of the source rock (tons/m^3).

During calculation of the SPI, 'ρ' for the MF samples is selected as 2.5 t/m^3 following the work by Peters and Cassa (1994).

Among the two informal subdivisions of the Mezardere Formation, the SPI values are calculated only for the UMF samples (Table 6). ORUs and their "h" values were

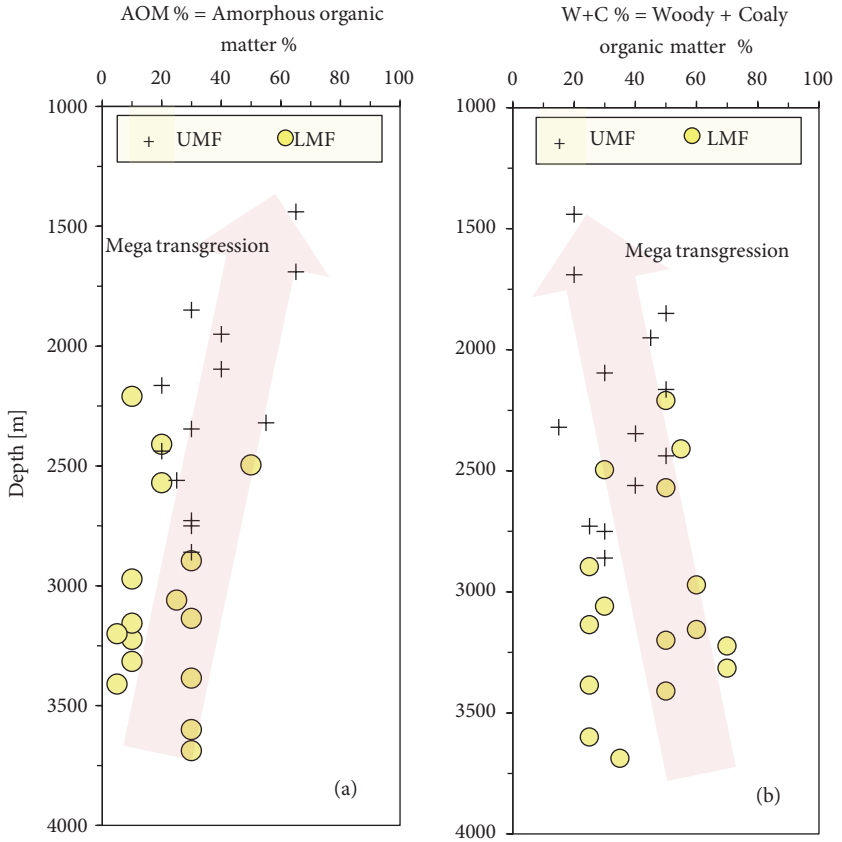

Figure 15. Maceral % vs. depth plots of the Lower Oligocene Mezardere Formation samples. (a) AOM % (amorphous organic matter %) versus depth and (b) (W+C) % {% (woody + coaly organic matter)} versus depth. Plots show increasing AOM % with decreasing depth in contrast decreasing W+C (%) by decreasing depth in "b" consistent to 'the sea level fluctuation' model proposed in this study.

Table 3. Descriptive statistic of the organic geochemical and petrographical parameters derived from (a) the Lower Mezardere Formation (LMF) ?Pshekian and (b) Upper Mezardere Formation (UMF) Solenovian samples. Descriptive statistic results are obtained from the data given in Table 2.

(a)	1	2	3	4	5	6	7	8	9	10	11	12	13	14	15	16	17
	Depth (m)	TOC	Tmax	HI	S1	S2	GP	PI	OSI	RHP	Vrcal	HOM	AOM	WOM	COM	W+C	% Ro
Valid cases	50	44	44	44	44	44	44	44	44	44	44	16	16	16	16	16	13
Mean	3077	0.88	435	136	0.21	1.32	1.53	0.16	23	1.66	0.67	35	20	35	10	44	0.64
Std. dev.	429	0.23	5	74	0.14	0.87	0.94	0.09	13	0.77	0.09	10	13	14	7	16	0.12
Minimum	2140	0.29	427	20	0.02	0.17	0.21	0.05	5	0.60	0.53	20	5	20	0	25	0.50
Maximum	3689	1.50	448	345	0.80	3.92	4.30	0.43	81	3.61	0.90	45	50	50	20	70	0.90
(b)	1	2	3	4	5	6	7	8	9	10	11	12	13	14	15	16	17
	Depth (m)	TOC	Tmax	HI	S1	S2	GP	PI	OSI	RHP	Vrcal	HOM	AOM	WOM	COM	W+C	% Ro
Valid cases	63	58	58	58	58	58	58	58	58	58	58	13	13	13	13	13	13
Mean	2297	1.15	431	285	0.16	3.52	3.69	0.05	13	2.98	0.60	29	37	28	6	34	0.51
Std. dev.	354	0.26	4	159	0.14	2.60	2.68	0.03	9	1.60	0.07	10	15	11	6	12	0.04
Minimum	1440	0.60	421	67	0.01	0.54	0.56	0.01	1	0.69	0.43	15	20	10	0	15	0.44
Maximum	2876	1.86	439	744	0.71	13.55	13.92	0.14	42	7.70	0.74	45	65	50	15	50	0.60

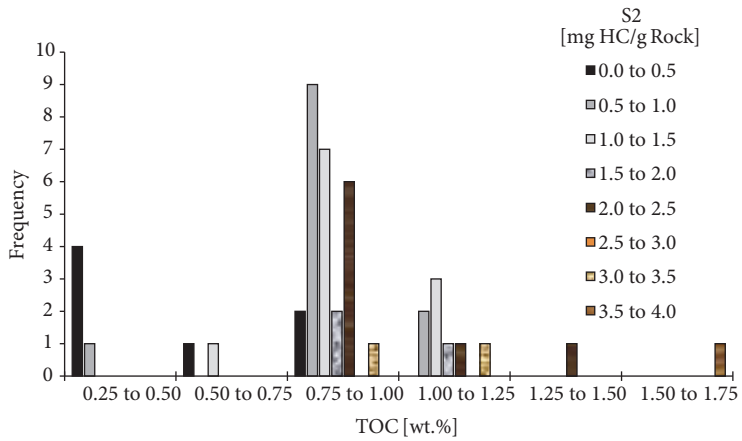

Figure 16. Ranges of TOC vs. frequency histogram associated with S2 values for the 44 Lower Mezardere Formation (LMF) samples.

determined with the help of the S1+S2 log curves, which were constructed separately for the four wells studied (Figures 21a–21d). During determination of the ORU thickness, only the points that provide GP = S1 + S2 > 2 mg HC/g rock condition were considered (Peters and Cassa, 1994). As a result, nine ORU intervals with different thicknesses are determined as shown in Figures 21a–21d and Table 6. Calculated SPI values of the nine ORU intervals are given in Table 6. Accordingly, K-A, K-B, U-C, and V-D wells have total SPI values of 2.25, 3.99, 1.20, and 5.51 tHC/m^2, respectively. These values are not compatible with the world's best source rocks. For example, an average SPI value of the Upper Permian source rocks of the Junggar Basin is 62.5 and Upper Jurassic source rock of the North Sea is 15 (Demaison and Huizinga, 1994). The average SPI value (5.51 tHC/m^2) of the UMF in the V-D well puts it into the moderate petroleum potential category of Demaison and Huizinga (1994) regardless of drainage system type (i.e. lateral or vertical drainage petroleum systems). Coeval units of the ORU intervals observed in the V-D well may have significant unconventional shale-oil potential even in the V-D well but in the more mature areas these ORU intervals may also act as an active conventional source rock.

5.4.3. Lower Oligocene Mezardere Formation as a source of the Gelindere oil

The Gelindere oil located in the southern part of the Thrace Basin (Figure 4) is the only oil that was generated from the Lower Oligocene MF (Gürgey, 2014). We think that the data we derived from this oil may have significant contributions to the depositional environmental interpretation of the MF. In the present study, we have already made some depositional environmental interpretation on the basis of palynological data, organic petrography, and geochemistry of the MF samples. Furthermore, n-alkanes (GC), high molecular weight n-alkanes and alkylcyclopentanes (HTGC), sterane and terpane biomarkers (GC-MS), and bulk (IRMS) and individual n-alkane (GC-IRMS) stable carbon isotope ratios ($\delta^{13}C$) of the Gelindere oil (Gürgey, 2014) are given here to support the environmental interpretations made in this study. Prediction of source rock characteristics using oil biomarkers (i.e. in terms of organic matter type, age, environment of deposition, lithology, and thermal maturity) is now a routine process in organic geochemistry (Moldowan et al., 1985; Philp, 1985; Waples and Machihara, 1990; Peters et al., 2005). In this respect, GC, HTGC, and GC-MS chromatograms of the Gelindere oil from Gürgey (2014) are given in Figures 22a–22d.

1- Low bioproductivity

· Low ααα sterane concentration (see page 52 in Gürgey, 2014). Low $C_{28}/(C_{27} + C_{29})$ sterane ratio = 0.25 from Figure 22c.

2- Continental organic matter

· Low HHI (C_{35} Homohopane index = 3% from Figure 22d). C_{35} HHI = $[(C_{35}$ (22S + 22R)/$C_{31} - C_{35}$ (22S + 22R)] × 100

3- Algal OM

· High nC_9–C_{15} alkane concentration (see Figure 22a).

4- Cenozoic age

· Presence of oleanane (see Figure 22d).

5- Coastal marine–estuarine depositional environment

· C_{27};C_{28};C_{29} distribution = 36;20;44 (see Figure 22c).

6- Dysoxic–oxic water redox conditions

· High pristane to phytane ratio = 2.39 > 1 (see Figure 22a).

· Pristane/nC_{17} vs. phytane/nC_{18} plot of Gürgey (2014) (see also Figure 22a).

Table 4. Pearson correlation coefficient (PCC) values between the organic geochemical and organic petrological parameters for the LMF samples. The data from which PCCs are calculated are given in Table 2. The PCC values greater than 0.50 are assumed to be significant.

		1	2	3	4	5	6	7	8	9	10	11	12	13	14	15	16	17
		Depth	TOC	Tmax	HI	S1	S2	GP	PI	OSI	RHP	VRcal	HOM	AOM	WOM	COM	W+C	%Ro
1	DEPTH	1.00																
	Valid cases	50																
2	TOC	–0.09	1.00															
	Valid cases	44	44															
3	Tmax	–0.43	–0.41	1.00														
	Valid cases	44	44	44														
4	HI	–0.59	0.47	0.01	1.00													
	Valid cases	44	44	44	44													
5	S1	–0.15	0.59	–0.24	0.31	1.00												
	Valid cases	44	44	44	44	44												
6	S2	–0.53	0.66	–0.05	0.92	0.40	1.00											
	Valid cases	44	44	44	44	44	44											
7	GP	–0.52	0.71	–0.08	0.90	0.53	0.99	1.00										
	Valid cases	44	44	44	44	44	44	44										
8	PI	0.54	0.03	–0.21	–0.55	0.38	–0.50	–0.41	1.00									
	Valid cases	44	44	44	44	44	44	44	44									
9	OSI	–0.06	0.35	–0.20	0.21	0.94	0.23	0.36	0.47	1.00								
	Valid cases	44	44	44	44	44	44	44	44	44								
10	RHP	–0.61	0.45	–0.01	0.93	0.40	0.93	0.93	–0.53	0.33	1.00							
	Valid cases	44	44	44	44	44	44	44	44	44	44							
11	VRcal	–0.43	–0.41	1.00	0.01	–0.24	–0.05	–0.08	–0.21	–0.20	–0.01	1.00						
	Valid cases	44	44	44	44	44	44	44	44	44	44	44						
12	HOM	0.30	0.66	–0.86	0.25	0.19	0.51	0.49	–0.14	0.06	0.39	–0.86	1.00					
	Valid cases	16	10	10	10	10	10	10	10	10	10	10	16					
13	AOM	–0.07	0.64	–0.80	0.09	0.37	0.35	0.38	0.26	0.26	0.28	–0.80	0.03	1.00				
	Valid cases	16	10	10	10	10	10	10	10	10	10	10	16	16				
14	WOM	–0.46	–0.54	0.78	0.10	–0.09	–0.21	–0.20	–0.24	0.03	–0.06	0.78	–0.69	–0.60	1.00			
	Valid cases	16	10	10	10	10	10	10	10	10	10	10	16	16	16			
15	COM	0.57	–0.61	0.59	–0.66	–0.55	–0.71	–0.74	0.35	–0.46	–0.77	0.59	–0.13	–0.61	0.11	1.00		
	Valid cases	16	10	10	10	10	10	10	10	10	10	10	16	16	16	16		
16	W + C	–0.13	–0.71	0.90	–0.19	–0.30	–0.47	–0.48	–0.06	–0.17	–0.36	0.90	–0.64	–0.78	0.89	0.55	1.00	
	Valid cases	16	10	10	10	10	10	10	10	10	10	10	16	16	16	16	16	
17	%Ro	0.75	–0.48	0.00	–0.74	–0.02	–0.87	–0.81	0.85	0.09	–0.83	0.00	0.30	–0.22	–0.38	0.65	0.01	1.00
	Valid cases	13	8	8	8	8	8	8	8	8	8	8	12	12	12	12	12	13

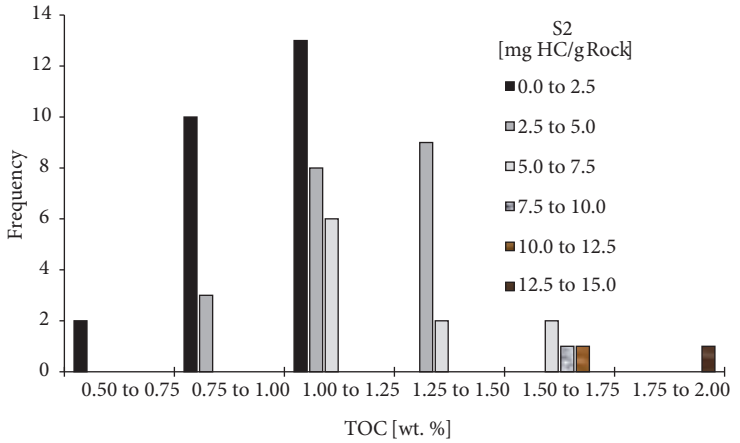

Figure 17. Ranges of TOC vs. frequency histogram associated with S2 values for the 58 Upper Mezardere Formation (UMF) samples.

Table 5. Pearson correlation coefficient (PCC) values among the organic geochemical and organic petrographical parameters for the UMF samples. The data from which PCCs are calculated are given in Table 2. The PCC values greater than 0.50 are assumed to be significant.

		1	2	3	4	5	6	7	8	9	10	11	12	13	14	15	16	17
		Depth	TOC	Tmax	HI	S1	S2	GP	PI	OSI	RHP	VRcal	HOM	AOM	WOM	COM	W+C	%Ro
1	Depth	1.00																
	Valid cases	63																
2	TOC	–0.46	1.00															
	Valid cases	58	58															
3	Tmax	–0.18	–0.05	1.00														
	Valid cases	58	58	58														
4	HI	–0.30	0.61	–0.15	1.00													
	Valid cases	58	58	58	58													
5	S1	–0.24	0.62	0.05	0.49	1.00												
	Valid cases	58	58	58	58	58												
6	S2	–0.46	0.76	–0.02	0.93	0.56	1.00											
	Valid cases	58	58	58	58	58	58											
7	GP	–0.46	0.77	–0.01	0.93	0.60	1.00	1.00										
	Valid cases	58	58	58	58	58	58	58										
8	PI	0.33	–0.05	0.07	–0.29	0.51	–0.29	–0.25	1.00									
	Valid cases	58	58	58	58	58	58	58	58									
9	OSI	–0.07	0.41	0.00	0.39	0.95	0.40	0.43	0.66	1.00								
	Valid cases	58	58	58	58	58	58	58	58	58								
10	RHP	–0.35	0.62	–0.11	0.97	0.52	0.96	0.95	–0.32	0.41	1.00							
	Valid cases	58	58	58	58	58	58	58	58	58	58							
11	Vcal	–0.18	–0.05	1.00	–0.15	0.05	–0.02	–0.01	0.07	0.00	–0.11	1.00						
	Valid cases	58	58	58	58	58	58	58	58	58	58	58						
12	HOM	0.94	–0.37	–0.07	–0.72	–0.31	–0.72	–0.71	0.38	–0.13	–0.67	–0.07	1.00					
	Valid cases	13	8	8	8	8	8	8	8	8	8	8	13					
13	AOM	–0.66	0.53	0.30	0.41	0.08	0.61	0.60	–0.50	–0.22	0.37	0.30	–0.60	1.00				
	Valid cases	13	8	8	8	8	8	8	8	8	8	8	13	13				
14	WOM	–0.21	–0.30	–0.15	0.25	–0.07	0.06	0.05	–0.18	0.05	0.22	–0.15	–0.27	–0.53	1.00			
	Valid cases	13	8	8	8	8	8	8	8	8	8	8	13	13	13			
15	COM	0.52	0.02	–0.26	–0.16	0.48	–0.25	–0.22	0.81	0.62	–0.11	–0.26	0.38	–0.63	0.01	1.00		
	Valid cases	13	8	8	8	8	8	8	8	8	8	8	13	13	13	13		
16	W + C	0.06	–0.30	–0.30	0.17	0.18	–0.07	–0.06	0.25	0.38	0.17	–0.30	–0.06	–0.76	0.88	0.48	1.00	
	Valid cases	13	8	8	8	8	8	8	8	8	8	8	13	13	13	13	13	
17	%Ro	0.79	–0.43	0.27	–0.47	–0.49	–0.56	–0.57	–0.04	–0.33	–0.50	0.27	0.67	–0.59	0.06	0.31	0.20	1.00
	Valid cases	13	8	8	8	8	8	8	8	8	8	8	13	13	13	13	13	13

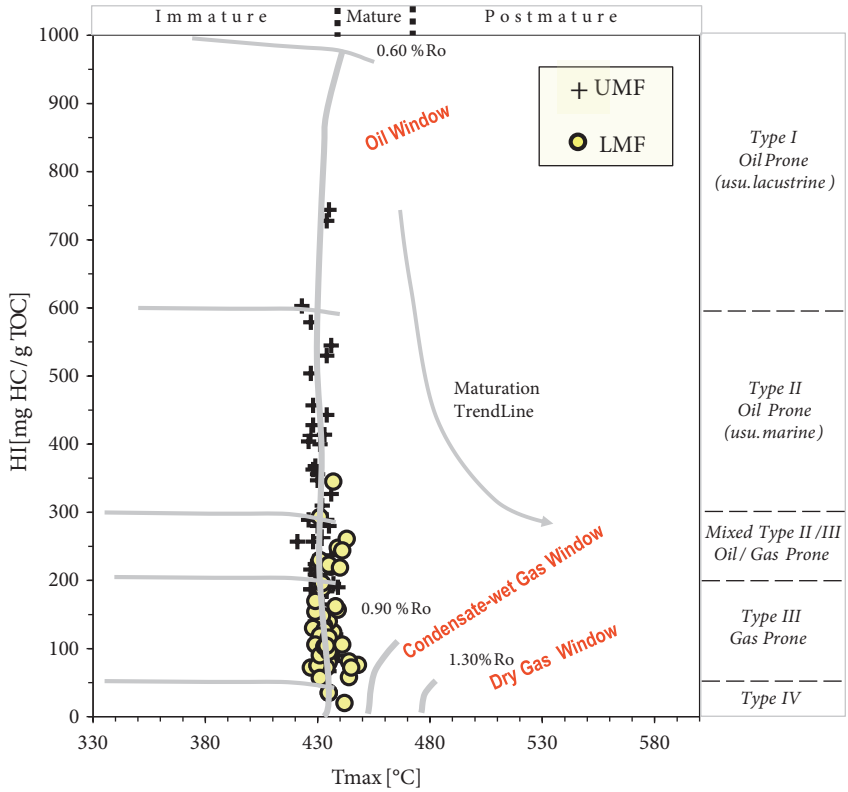

Figure 18. HI vs. Tmax plot showing great variation in HI values with very slight changing in Tmax (maturity) values. This phenomenon is probably related to the sea level fluctuations during the deposition of the Lower Oligocene Mezardere Formation.

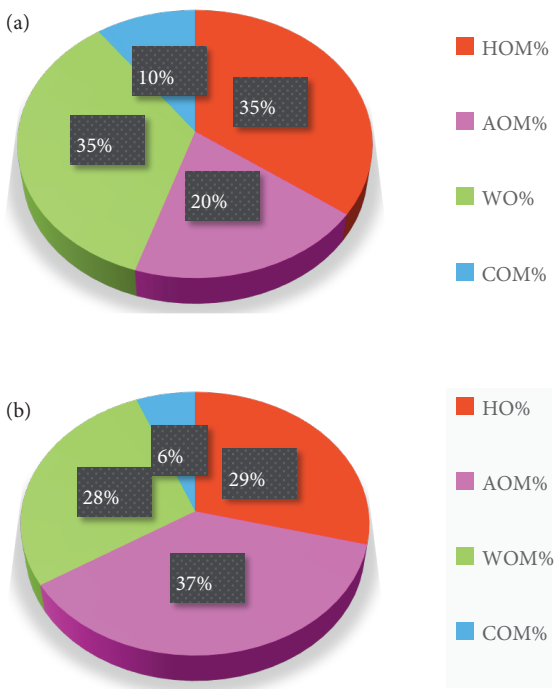

Figure 19. (a) Pie diagram of the maceral % distribution in the Lower Mezardere Formation (LMF) and (b) for the Upper Mezardere Formation (UMF) samples.

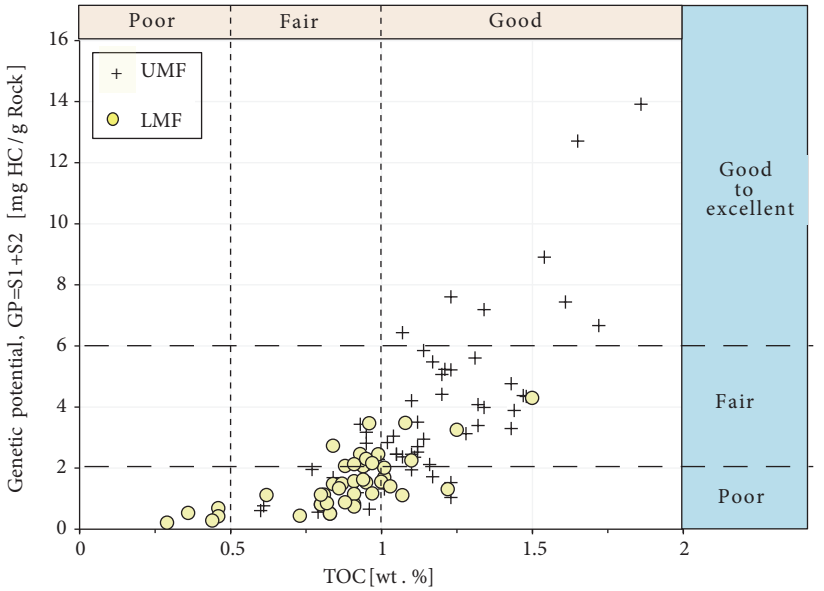

Figure 20. Genetic potential (S1+S2) vs. TOC plot of the Lower Oligocene Mezardere Formation samples.

Table 6. Selected organic-rich units (ORUs) from the Upper Mezardere (UMF) intervals in the four wells studied. Their genetic potential (GP) and the source potential indexes (SPI) are given. Positions of the ORUs along the wells are shown in Figures 21a–21d. Location of the wells are given in Figure 4 (K-A = Karacaoglan-A; K-B = Kumrular-B; U-C = Umurca-C; V-D = Vakiflar-D wells).

Well name	Organic-rich unit (ORU)	Top (m)	Base (m)	Net thickness (m)	GP = S1 + S2 (mg HC/g rock)	Density (t/m^3)	SPI (tHC/m^2)
K-A	UM-ORU-1	1900	2010	110	3.20	2.5	0.88
K-A	UM-ORU-2	2115	2265	150	3.65	2.5	1.37
Total							2.25
K-B	UM-ORU-1	1650	1810	160	7.56	2.5	3.02
K-B	UM-ORU-2	1925	2015	90	4.33	2.5	0.97
Total							3.99
U-C	UM-ORU-1	2257	2350	93	3.00	2.5	0.70
U-C	UM-ORU-2	2575	2665	90	2.23	2.5	0.50
Total							1.20
V-D	UM-ORU-1	2055	2150	95	3.40	2.5	0.81
V-D	UM-ORU-2	2200	2610	410	3.98	2.5	4.08
V-D	UM-ORU-3	2675	2745	70	3.53	2.5	0.62
Total							5.51

7- Freshwater input into the depositional side

· Presence of C_{30} 4 methyl steranes (see Figure 22c).

· $CPI_{42-46} < 1$ (0.97) (CPI = Carbon Preference Index (see Figure 22b).

· $CPI_{42-46} = [2 (C_{43} - C_{45})]/[(C_{44} + C_{46}) + (C_{42} + C_{44})]$

· Negative slope of $\delta^{13}C$ individual nC_9–nC_{19} alkanes (see page 62 and Figure 11 of Gürgey, 2014).

8- Clastic lithology

· Low C_{29} norhopane/C_{30} hopane ratio = 0.44 (see Figure 22d).

9- Low thermal maturity of 0.50–0.60 %Ro

· 22S/(22S + 22R) ratio = 0.60 (see Figure 22d).

Depositional environmental characteristics of the source rock of the Gelindere oil given above are compared

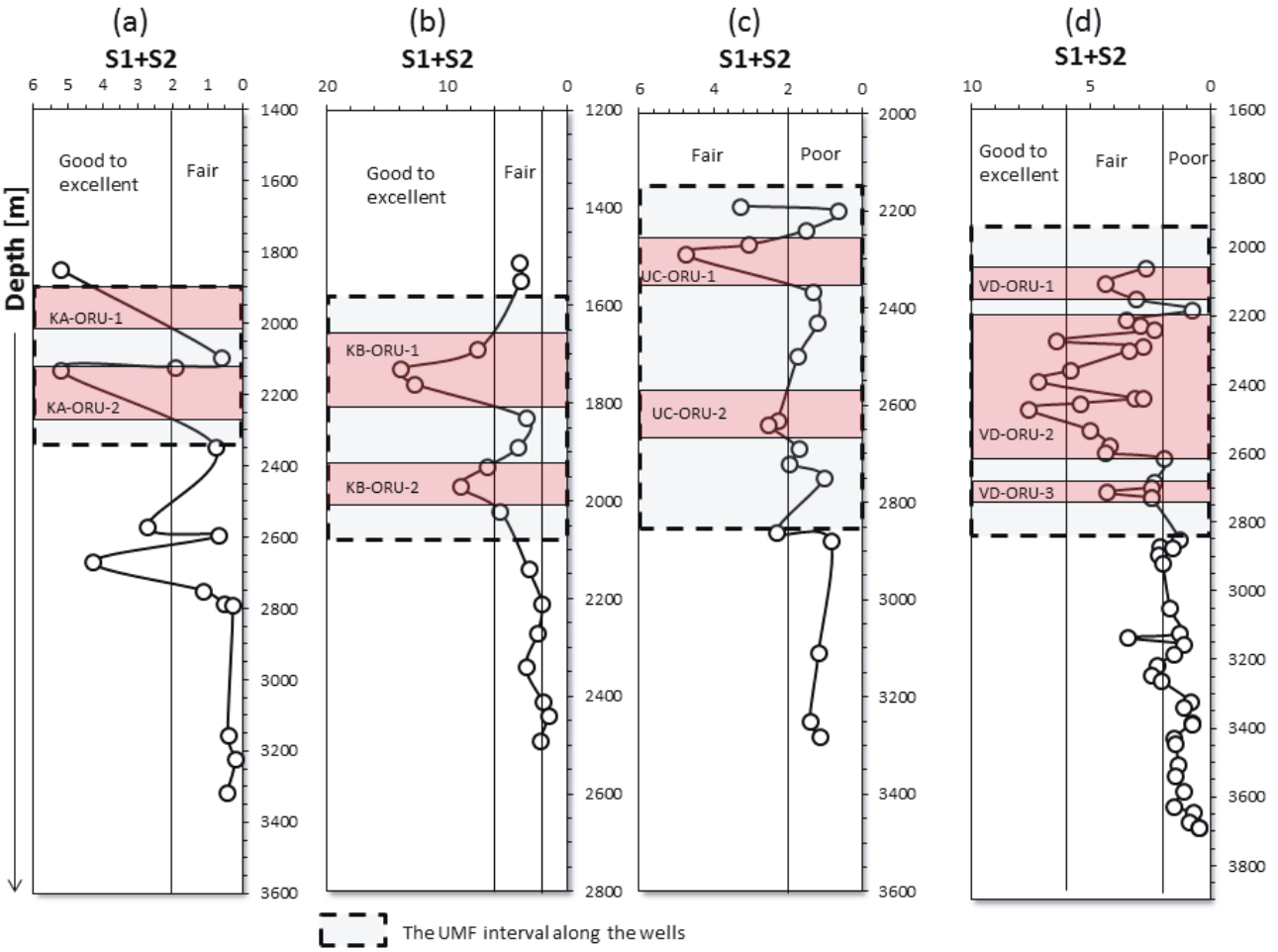

Figure 21. Genetic potential (S1+S2) log curves for the four wells studied.

to those of the UMF and the LMF. We conclude that the Gelindere oil could be derived from the UMF. If so, this has several implications for hydrocarbon exploration in the Thrace Basin. One of these is that the future mass balance studies between the amount of discovered oil and the generated oil from the source rock should consider the UMF instead of the whole thickness of the MF. Secondly, unconventional shale-oil studies should be focused on the UMF since it has sufficient organic richness, the right type of organic matter, and has reasonable maturity (Gürgey, 2015).

6. Conclusions

1. The Mezardere Formation, for the first time, is informally subdivided into the ?Pshekian Lower Mezardere Formation based on the common occurrences of *Glaphyrocysta* cf. *semitecta* and absence of *Wetzeliella gochtii* corresponding to ?NP21/22 zones and the Solenovian Upper Mezardere Formation based on the very rich and diverse dinocyst assemblage having abundant occurrences of age-diagnostic *Wetzeliella gochtii* and corresponding to NP23/24 zones. This informal subdivision is consistent with the vertical distribution of the organic geochemical data and it allowed us to compare various geochemical properties of the Mezardere Formation with coeval deposits in the Eastern Paratethys realm.

2. The depositional environment of the Mezardere Formation has changed from neritic normal-marine in the ?Pshekian to shallower neritic brackish-marine in the Solenovian. Higher abundances of *Pediastrum* spp. identified for the first time in the Upper Mezardere Formation were interpreted as an indication of freshwater input during Solenovian in the Thrace Basin. Similar observations indicating a heavy freshwater influx were made by European scientists based on richness in nutrients and nannoplankton blooms in the Eastern and Western Paratethys.

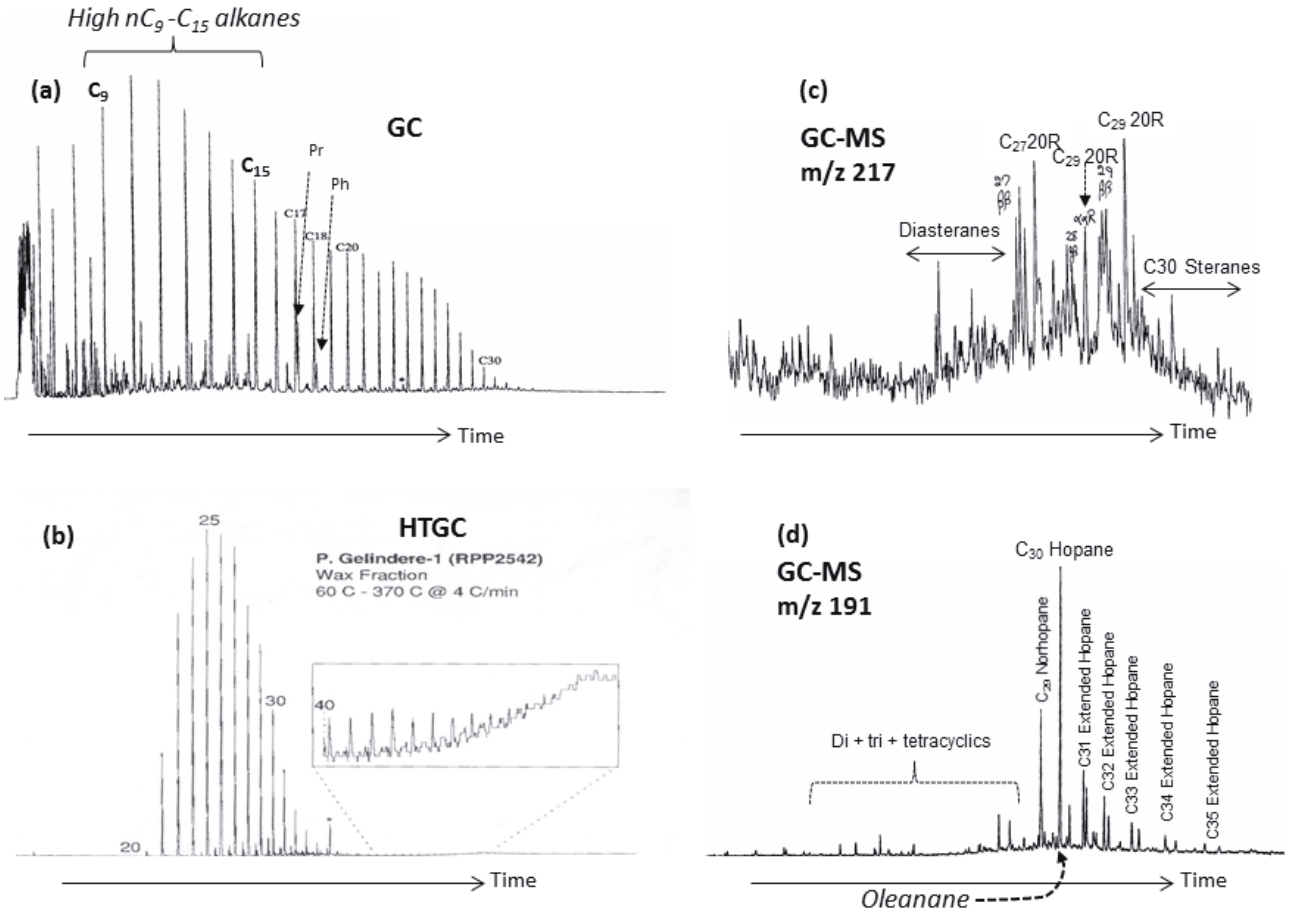

Figure 22. Gas chromatogram (a), HTGC (b), m/z 217 sterane (c), and m/z 191 terpane (d) mass chromatograms of the Lower Oligocene Mezardere Formation-sourced Gelindere oil located in the southern Thrace Basin (Gürgey, 2014). See Figures 1 and 4 for the location of Gelindere oil.

3. Organic geochemical proxies (i.e. TOC, HI, and RHP) indicate that there are three relatively short-term transgressive-regressive high order cycles during the deposition of the Mezardere Formation.

4. Characterized by relatively high source rock and hydrocarbon potential, the Solenovian Upper Mezardere Formation corresponds to cycle - 3 and marks the time of transgression, which is a function of maximum and drastic rise of sea level. Its SPI in the K-A, K-B, U-C, and V-D wells is 2.25, 3.99, 1.20, and 5.51 t HC/m^2, respectively. SPI was not calculated for the ?Pshekian Lower Mezardere Formation samples due to its low Rock-Eval TOC, HI, and S2 values.

Acknowledgments

We are grateful to Mr Haki Naz and Dr Nazım Özgür Sipahioğlu for their valuable support to review and improve the quality of the paper with critical remarks. We are indebted to Reyhan Kara Gülbay and the anonymous reviewers for their comments and constructive suggestions, which contributed to the quality of this paper. Finally, we are thankful for the Turkish Petroleum Corporation's permission to publish this research.

References

Abouelresh MO, Slatt RM (2012). Lithofacies and sequence stratigraphy of the Barnett Shale in east-central Fort Worth Basin, Texas. AAPG Bull 96: 1-22.

Barker C (1974). Pyrolysis techniques for source rock evaluation. AAPG Bull 58: 2349-2361.

Barski M, Bojanowski M (2010). Organic-walled dinoflagellate cysts as a tool to recognize carbonate concretions: an example from Oligocene flysch deposits of the Western Carpathians. Geol Carpath 61: 121-128.

Batı Z (1996). Palynostratigraphy and coal petrography of the Upper Oligocene lignites of the Northern Thrace Basin, NW Turkey. PhD, Middle East Technical University, Ankara, Turkey.

Bati Z (2015). Dinoflagellate cyst biostratigraphy of the upper Eocene and lower Oligocene of the Kirmizitepe Section, Azerbaijan, South Caspian Basin. Rev Palaeobot Palyno 217: 9-38.

Batı Z, Erk S, Akça N (1993). Trakya Havzası Tersiyer birimlerinin palinomorf, foraminifer ve nannoplankton biyostratigrafisi. TPAO Rep No: 1947, Ankara, Turkey: TPAO (in Turkish).

Batı Z, Pinçe S, Akça, N (2007). Biostratigraphical properties of the Priabonian-Rupelian (Upper Eocene-Lower Oligocene) boundary in the Thrace Basin. In: Abstracts of Turkish Stratigraphy Committee Workshop, MTA, Ankara, Turkey, pp. 14.

Bati Z, Sancay RH (2007). Palynostratigraphy of Rupelian sediments in the Muş Basin, Eastern Anatolia, Turkey. Micropaleontology 53: 249-283.

Bechtel A, Hamor-Vido M, Gratzer R, Sachsenhofer RF, Pütmann W (2012). Facies evolution and stratigraphic correlation in the early Oligocene Tard Clay of Hungary as revealed by maceral, biomarker and stable isotope composition. Mar Petrol Geol 35: 55-74.

Bechtel A, Movsumova U, Strobl SAI, Sachsenhofer RF, Soliman A, Gratzer R, Püttmann W (2013). Organofacies and paleoenvironment of the Oligocene Maikop series of Angeharan (eastern Azerbaijan). Org Geochem 56: 51-67.

Bechtel A, Movsumova U, Pross J, Gratzer R, Coric S, Sachsenhofer RF (2014). The Oligocene Maikop series of Lahich (eastern Azerbaijan): Paleoenvironment and oil-source correlation. Org Geochem 71: 43-59.

Brinkhuis H, Biffi U (1993). Dinoflagellate cyst stratigraphy of the Eocene/Oligocene transition in Central Italy. Mar Micropaleontol 22: 131-183.

Bürkan K (1992). Geochemical evaluation of the Thrace Basin. In: Proceedings of the 9th Petroleum Congress of Turkey, Proceedings, Ankara, Turkey, pp. 34-48 (article in Turkish with an abstract in English).

Coccioni R, Marsili A, Montanari A, Belanca A, Neri R, Bice DM, Brinkhuis H, Church N, Macalady A, McDaniel A et al (2008). Integrated stratigraphy of the Oligocene pelagic sequence in the Umbria-Marche basin (northeastern Apennines, Italy): a potential Global stratotype Section and Point (GSSP) for the Rupelian/Chattian boundary. Geo Soc Am Bull 120: 487-511.

Costa LI, Downie C (1976). The distribution of the dinoflagellate Wetzeliella in the Palaeogene of North-Western Europe. Palaeontology 19: 591-614.

Creaney S, Passey RQ (1993). Recurring patterns of total organic carbon and source rock quality within a sequence stratigraphic framework. AAPG Bull 77: 386-401.

Curiale AJ, Cole DR, Witmer J (1992). Application of organic geochemistry to sequence stratigraphic analysis: Four Corners Platform Area, New Mexico, U.S.A. Org Geochem 19: 53-75.

Demaison GJ, Moore G T (1980). Anoxic environments and oil source bed genesis. AAPG Bull 64: 1179-1209.

Demaison G, Huizinga B (1994). Genetic classification of petroleum systems using three factors; charge, migration, and entrapment, In: Magoon LB, Dow WG, editors. Petroleum System-From Source to Trap. Tulsa, OK, USA: AAPG Memoir 60: pp. 73–89.

Dybkær K (2004). Dinocyst stratigraphy and palynofacies studies used for refining a sequence stratigraphic model-uppermost Oligocene to lower Miocene, Jylland, Denmark. Rev Palaeobot Palyno 131: 201-249.

Ediger VŞ, Alişan C (1989). Tertiary fungal and algal palynomorph biostratigraphy of the northern Thrace basin, Turkey. Rev Palaeobot Palyno 58: 139-161.

Ediger VŞ, Bati Z (1988). Morphological examination of Pediastrum (Chlorophyta) from the Tertiary strata of the Thrace basin (NW Turkey). Pollen et Spores 30: 203-222.

Eldrett JS, Harding IC, Firth JV, Roberts AP (2004). Magnetostratigraphic calibration of Eocene-Oligocene dinoflagellate cyst biostratigraphy from the Norwegian-Greenland Sea. Mar Geol 204: 91-127.

Erten T, Çubukçu A (1988). K. Trakya havzası Eosen-Oligosen yaşlı çökellerin petrografik, sedimantolojik özellikleri, tektonik ortamsal modelleri. TPAO Rep No: 1217, Ankara, Turkey: TPAO (in Turkish).

Fang H, Jianyu C, Yongchuan S, Yaozong L (1993). Application of organic facies studies to sedimentary basin analysis: a case study from the Yitong Graben, China. Org Geochem 20: 27-47.

Freire MFA, Monteiro CM (2013). A novel approach for infring the proportion of terrestrial organic matter input to marine sediments on the basis of TOC, TN and δ13Corg signatures. Open Journal of Marine Science 3: 74-92.

Gedl P (2004). Dinoflagellate cysts from the Šambron beds (Central Carpathian Palaeogene) in Lovak Orava. Studia Geologica Polonica 123: 223-243.

Gradstein FM, Ogg JG, Smith AG (editors) (2004). Geologic time scale (Neogene-Late Oligocene). 1st ed. Cambrigde, UK: Cambridge University Press.

Gültekin AH (1998). Geochemistry and origin of of the Oligocene Binkılıç Manganese deposits, Thrace basin, Turkey. Turkish J Earth Sci 7: 11-24.

Gürgey K (1999). Geochemical characteristic and thermal maturity of oils from the Thrace Basin (western Turkey) and western Turkmenistan. J Petrol Geol 22: 167-189.

Gürgey K (2013). Lower Oligocene Mezardere Formation as an unconventional shale-oil system: prospective area likely to be suitable for oil field development, Thrace Basin. In: Abstracts and Proceedings of the 19th International Petroleum and Natural Gas Congress and Exhibition of Turkey, Ankara, Turkey, pp. 359-361.

Gürgey K (2014). Oil-oil and oil-source rock correlation in the Tertiary Thrace Basin, NW Turkey. TAPG Bulletin 26: 47-69.

Gürgey K (2015). Estimation of oil in-place resources in the lower Oligocene Mezardere Shale, Thrace Basin, Turkey. J Petrol Sci Eng 133: 543-565.

Gürgey K, Philp RP, Clayton C, Emiroğlu H, Siyako M (2005). Geochemical and isotopic approach to maturity/source/mixing estimations for natural gas and associated condensates. Appl Geochem 20: 2017-2037.

Habib D, Miller JA (1989). Dinoflagellate species and organic facies evidence of marine transgression and regression in the Atlantic Coastal Plain. Palaeogeogr Palaeoecl 74: 23-47.

Haq BU, Hardenbol J, Vail RP (1987). Chronology of fluctuating sea levels since the Triassic. Science 235: 1156-1167.

Haq BU, Hardenbol J, Vail PR (1988). Mesozoic and Cenozoic chronostratigraphy and cycles of sea level change. In: Wilgus CK, Hasting BS, Kendal CGStC, Posamentier HW, Ross CA, Van Wagoner JC, editors. Sea-level Changes, an Integrated Approach. Houston, TX, USA: Soc Econ Pa, Special Publications 42: pp. 71-108.

Harput B, Gökçen SL (1991). Application of organic facies method in the Thrace Basin. Sediment Geol 72: 171-187.

Hart GF, Pasley MA, Gregory WA (1994). Particulate organic matter, maceral facies models and application to sequence stratigraphy. In: Travese A, editor. Sedimentation of Organic Particles. Cambridge, UK: Cambridge University Press, pp. 337-390.

Hoşgörmez H, Yalçın MN, Cramer B, Gerling P, Mann U (2005). Molecular isotopic composition of gas occurrences in the Thrace Basin (Turkey). Origin of the gases and characteristics of possible source rocks. Chem Geol 214: 179-191.

İslamoğlu Y, Harzhauser M, Gross M, Jimenez-Moreno G, Coric S, Kroh A, Rögl F, Van MJ (2008). From Tethys to Eastern Paratethys: Oligocene depositional environments, paleoecology and paleobiogeography of the Thrace Basin (NW Turkey). Int J Earth Sci 99: 183-200.

Jaramillo CA, Oboh-Ikuenobe FE (1999). Sequence stratigraphic interpretations from palynofacies, dinocyst and lithological data of Upper Eocene-Lower Oligocene strata in southern Mississippi and Alabama, U.S. Gulf Coast. Palaeogeogr Palaeocl 145: 259-302.

Jarvie DM, Morelos A, Han Z (2001). Detection of pay zones and pay quality. Gulf of Mexico: application of geochemical techniques. Gulf Coast Association of Geological Societies Transactions 51: 151-160.

Jones RW (1987). Organic facies. In: Brooks J, Welte HD, editors. Advances in Petroleum Geochemistry (2). London, UK: Academic Press, pp. 1-90.

Köthe A (1990). Paleogene dinoflagellates from Northwest Germany-biostratigraphy and paleoenvironment. Geol Jb A 118: 3-111.

Köthe A, Piesker B (2007). Stratigraphic distribution of Paleogene and Miocene dinocysts in Germany. Revue de Paléobiologie Genève 26: 1-39.

Liengjarern M, Costa L, Downie C (1980). Dinoflagellate cysts from the Upper Eocene-Lower of the Isle of Wight. Palaeontology 23: 475-499.

Linda CI, Nesbitt EA, Prothero DR (2003). The marine Eocene-Oligocene transition: a synthesis. In: Prothero DR, Ivany LC, Nesbitt EA, editors. From Greenhouse to Icehouse, New York, NY, USA: Columbia University Press, pp. 522-534.

Miceli-Romero A, Philp PR (2012). Organic geochemistry of the Woodford Shale, southeastern Oklahoma: how variable can shales be? AAPG Bull 96: 493-517.

Moldowan JM, Seifert WK, Gallegos EJ (1985). Relationship between petroleum composition and depositional environment of petroleum source rocks. AAPG Bull 69: 1255-1268.

Omura A, Hoyanaki K (2004). Relationship between composition of organic matter, depositional environments, and sea-level changes in backarc basins, Central Japan. J Sediment Res 74: 620-630.

Öztürk H, Frakes AL (1995). Sedimentation and diagenesis of an Oligocene manganese deposit in a shallow subbasin of the Paratethys: Thrace Basin, Turkey. Ore Geol Rev 10: 117-132.

Pasley MA, Gregory AW, Hart FG (1991). Organic matter variations in transgressive and regressive shales. Org Geochem 17: 483-509.

Pasley MA, Hazel JE (1990). Use of organic petrology and graphic correlation of biostratigraphic data in sequence stratigraphic interpretations: examples from the Eocene-Oligocene boundary section, St. Stephens Quarry, Alabama. Gulf Coast Associations of Geological Societies Transactions 40: 661-683.

Perinçek D (1991). Possible strand of the North Anatolian Fault in the Thrace Basin, Turkey - an interpretation. AAPG Bull 75: 241-257.

Peters KE (1986). Guidelines for evaluating petroleum source rock using programmed pyrolysis. AAPG Bull 70: 318-329.

Peters KE, Moldowan MJ (1991). Effects of source, thermal maturity, and biodegradation on the distribution and isomerization of homohopanes in petroleum. Org Geochem 49: 47-61.

Peters KE, Cassa MR (1994). Applied source rock geochemistry. In: Magoon LB, Dow WG, editors. Petroleum System-From Source to Trap. Tulsa, OK, USA: AAPG Memoir 60: pp. 93-120.

Peters KE, Walters CC, Moldowan CM (2005). The Biomarker Guide. 2nd ed. Cambridge, UK: Cambridge University Press.

Philp PR (1985). Fossil Fuel Biomarkers - Applications and Spectra. Methods in Geochemistry and Geophysics 23. Amsterdam, the Netherlands: Elsevier.

Popov SV, Akhmetiev MA, Zaporozhets NI, Voronina AA, Stolyarov AS (1993). Evolution of Eastern Paratethys in the Late Eocene-Early Miocene. Stratigr Geol Correl 1: 10-39.

Popov SV, Antipov PM, Zastrozhnov SA, Kurina EE, Pinchuk NT (2010). Sea level fluctuations on the Northern shelf of the Eastern Paratethys in the Oligocene-Neogene. Strat Geol Correl 18: 200-224.

Popov SV, Rögl F, Rozanov AY, Steininger FF, Scherba IG, Kovac M (2004). Lithological- paleogeographic maps of the Pratethys (10 maps Late Eocene to Pliocene). Courier Forschungsinstitut Senckenberg 250: 1-46.

Popov SV, Stolyarov AS (1996). Paleogeography and anoxic environments of the Oligocene-Early Miocene eastern Paratethys. Israel J Earth Sci 45: 161-167.

Powell AJ (1992). Dinoflagellate cysts of the Tertiary System. In: Powell AJ, editor. A Stratigraphic Index of the Dinoflagellate Cysts. 1st ed. London, UK: Chapman & Hall, pp. 155-252.

Pross J (2001). Dinoflagellate cyst biogeography and biostratigraphy as a tool for palaeoceanographic reconstructions: An example from the Oligocene of western and northwestern Europe. Neues Jahrb Geol P -A 219: 207-219.

Pross J, Brinkhuis H (2005). Organic-walled dinoflagellate cysts as paleoenvironmental indicators in the Paleogene; a synopsis of concepts. Palaont Z 79: 53-59.

Pross J, Houben AJP, Van Simaeys S, Williams GL, Kotthoff U, Coccioni R, Wipshaar M, Brinkhuis H (2010). Umbria-Marche revisited: a refined magnetostratigraphic calibration of dinoflagellate cyst events for the Oligocene of the Western Tethys. Rev Palaeobot Palyno 158: 213-235.

Robinson AG, Rudat HJH, Banks CJ, Wiles RLF (1996). Petroleum geology of the Black Sea. Mar Petrol Geol 13: 195-223.

Rögl F (1998). Paleogeographic considerations for Mediterranean and Paratethys Seaways (Oligocene to Miocene). Annalen des Naturhistorischen Museums in Wien 99: 279-310.

Rögl F (1999). Mediterranean and Paratethys. Facts and hypotheses of an Oligocene to Miocene Paleogeography (Short Overview). Geol Carpath 50: 339-349.

Sachsenhofer RF, Bechtel A, Ćorić S, Georgiev G, Linzer HG, Gratzer R, Reischenbacher D, Schulz HM, Soliman A (2011). Lithology and Hydrocarbon Potential of Lower Oligocene Successions in the Alpine Foreland Basin: Model for Source Rocks in the Paratethys? Search and Discovery Article #10318.

Sachsenhofer RF, Hentschke J, Bechtel J, Ćorić S, Gratzer R, Gross D, Horsfield B, Rachetti A, Soliman A (2015). Hydrocarbon potential and depositional environments of Oligo-Miocene rocks in the Eastern Carpathians (Vrance nappe, Romania). Mar Petrol Geol 68: 269-290.

Sachsenhofer RF, Leitner B, Linzer HG, Bechtel A, Ćorić S, Gratzer R, Reischenbacher D, Soliman A (2010). Deposition, erosion and hydrocarbon source rock potential of the Oligocene Eggerding Formation (Molasse Basin, Austria). Austrian J Earth Sci 103: 76-99.

Sachsenhofer RF, Popov SY, Akhmediev MA, Betchel A, Gratzer R, Grob D, Horsfield B, Rachetti A, Rupprecht B, Schaffar WBH, Zaporozhets NI (2017). The type section of the Maikop Group (Oligocene-lower Miocene) at the Belaya River (North Caucasus): Depositional environment and hydrocarbon potential. AAPG Bull 101: 289-319.

Sachsenhofer RF, Stummer B, Georgiev G, Dellmour R. Bechtel A, Gratzer R, Coric C (2009). Depositional environment and hydrocarbon potential of the Oligocene Ruslar Formation (Kamchia depression; Western Black Sea). Mar Petrol Geol 26: 57-84.

Saint-Germés M, Bocherens H, Baudin F, Bazhenova O (2000). Evaluation of the δ13C values of organic matter of the Maykop series during Oligocene-Lower Miocene. B Soc Geol Fr 171: 13-21.

Sancay RH (2005). Palynostratigraphic and palynofacies investigation of the Oligocene-Miocene units in the Kars-Erzurum-Muş sub-basins (Eastern Anatolia). PhD, Middle East Technical University, Ankara, Turkey.

Sancay RH, Bati Z, Edwards LE, Ertug KI (2006a). A new species of *Pentadinium* from eastern Anatolia, Turkey, *Pentadinium galileoi*. Micropaleontology 52: 537-543.

Sancay RH, Batı Z, Işık U, Kırıcı S, Akça N (2006b). Palynomorph, foraminifera, and calcareous nannoplankton biostratigraphy of Oligo–Miocene sediments in the Muş Basin, Eastern Anatolia, Turkey. Turkish J Earth Sci 15: 259-319.

Schulz HM, Bechtel A, Rainer T, Sachsenhofer RF, Struck U (2004). Paleoceanography of the western central Paratethys during Early Oligocene nannoplankton zone NP23 in the Austrian Molasse Basin. Geol Carpath 55: 311-323.

Schulz HM, Bachtel A, Sachsenhofer RF (2005). The birth of the Paratethys during Early Oligocene: From Tethys to a Black sea analogue. Global Planet Change 49: 163-176.

Siyako M (2006). Trakya Havzası Tersiyer Kaya Birimleri. In: Trakya Bölgesi Litostratigrafi Birimleri. Stratigrafi Komitesi Litostratigrafi Birimleri Serisi-2. Ankara, Turkey: MTA, pp. 43-83 (in Turkish).

Siyako M, Huvaz O (2007). Eocene stratigraphic evolution of the Thrace Basin. Sediment Geol 198: 75-91.

Slatt MR, Rodriguez DN (2012). Comparative sequence stratigraphy and organic geochemistry of gas shales: commonality or coincidence? J Nat Gas Sci Eng 8: 68-84.

Sluijs A, Pross J, Brinkhuis H (2005). From greenhouse to icehouse; organic-walled dinoflagellate cysts as paleoenvironmental indicators in the Paleogene. Earth Sci Rev 68: 281-315.

Soliman A (2012). Oligocene dinoflagellate cysts from the North Alpine Foreland Basin: new data from the Eggerding formation (Austria). Geol Carpath 63: 49-70.

Song J, Littke R, Maquil R, Weniger P (2014). Organic facies variability in the Posidonia Black Shale from Luxemburg: implications for thermal maturation and depositional environment. Palaeogeogr Palaeocl 410: 316-336.

Soylu C, Harput B, İlleez, IH, Ertürk O, İztan H, Uğur F, Göker T, Harput A, Bizim Y, Gürgey K, et al (1992). Organic geochemical evaluation of the northern Thrace Basin. In: Proceedings of 9th Petroleum Congress of Turkey, Ankara, Turkey, pp. 49-61.

Tissot BP, Welte HD (1984). Petroleum Formation and Occurrence. New York, NY, USA: Springer-Verlag.

Torricelli S, Biffi U (2001). Palynostratigraphy of the Numidian flysch of North Tunisia (Oligocene-Early Miocene). Palynology 25: 29-55.

Turgut S, Eseller G (2000). Sequence stratigraphy, tectonics and depositional history of eastern Thrace Basin, NW Turkey. Mar Petrol Geol 17: 61-100.

Turgut S, Türkaslan M, Perinçek D (1991). Evaluation of the Thrace sedimentary basin and its hydrocarbon prospectivity. In: Spencer AM, editor. Generation, Accumulation, and Production of Europe's Hydrocarbons. Oxford, UK: Oxford University Press, EAPG Special Publications 1: pp. 415-437.

Van Simaeys S, Munsterman D, Brinkhuis H (2005). Oligocene dinoflagellate cyst biostratigraphy of the southern North Sea Basin. Rev Palaeobot Palyno 134: 105-128.

Varentsov IM (2002). Genesis of the eastern Paratethys manganese ore giants. Impact of events at the Eocene/Oligocene boundary. Ore Geol Rev 20: 65-82.

Varentsov IM, Muzyliov NG, Nikolaev VG, Stupin SI (2003). The origin of black shale-hosted Mn deposits in Paratethyan basins: constraints from geological events at the Eocene/Oligocene boundary. Russian Journal of Earth Sciences 5: 255-272.

Vetö I (1987). An Oligocene sink for organic carbon: upwelling in the Paratethys. Palaeogeogr Palaeocl 60: 143-153.

Waples DW, Machihara T (1990). Application of sterane and triterpene biomarkers in petroleum exploration. Bull Can Petrol Geol 38: 357-380.

Williams GL, Brinkhuis H, Pearce MA, Fensome RA, Weegink JW (2004). Southern Ocean and global dinoflagellate cyst events compared: Index events for Late Cretaceous-Neogene. In: Exon NF, Kennett JP, Malone MJ, editors. Proceedings of the Ocean Drilling Program, Scientific Results 189: College Station TX (Ocean Drilling Program), pp. 1-98.

Wilpshaar M, Santarelli A, Brinkhuis H, Visscher H (1996). Dinoflagellate cysts and mid-Oligocene in the central Mediterranean region. Journal of Geological Society London 153: 553-561.

Zaporozhets NI (1999). Palynostratigraphy and Dinocyst Zonation of the Middle Eocene-Lower Miocene Deposits at the Belaya River (Northern Caucasus). Stratigr Geol Correl 7: 161-178.